

# Robust Cooperative Manipulation without Force/Torque Measurements: Control Design and Experiments

Christos K. Verginis, *Member, IEEE*, Matteo Mastellaro, and Dimos V. Dimarogonas, *Member, IEEE*

**Abstract**—This paper presents two novel control methodologies for the cooperative manipulation of an object by  $N$  robotic agents. Firstly, we design an adaptive control protocol which employs quaternion feedback for the object orientation to avoid potential representation singularities. Secondly, we propose a control protocol that guarantees predefined transient and steady-state performance for the object trajectory. Both methodologies are decentralized, since the agents calculate their own signals without communicating with each other, as well as robust to external disturbances and model uncertainties. Moreover, we consider that the grasping points are rigid, and avoid the need for force/torque measurements. Load sharing coefficients are also introduced to account for potential differences in the agents' power capabilities. Finally, simulation and experimental results with two robotic arms verify the theoretical findings.

**Index Terms**—cooperative manipulation, multi-agent systems, adaptive control, robust control, unit quaternions, prescribed performance control.

## I. INTRODUCTION

MULTI-agent systems have gained significant attention the last years due to the numerous advantages they yield with respect to single-agent setups. In the case of robotic manipulation, heavy payloads and challenging maneuvers necessitate the employment of multiple robotic agents. Although collaborative manipulation of a single object, both in terms of transportation (regulation) and trajectory tracking, has been considered in the research community the last decades, there still exist several challenges that need to be taken account by on-going research, both in control design as well as experimental evaluation.

Early works develop control architectures where the robotic agents communicate and share information with each other, and completely decentralized schemes, where each agent uses only local information or observers, avoiding potential communication delays (see, indicatively, [1]–[10]). Impedance and hybrid force/position control is the most common methodology used in the related literature [8]–[24], where a desired impedance behavior is imposed potentially with force regulation. Most of the aforementioned works employ force/torque

sensors to acquire feedback of the object-robots contact forces/torques, which however may result to performance decline due to sensor noise or mounting difficulties. Force/Torque sensor-free methodologies can be found in [6], [8], [16], which have inspired the dynamic modeling in this work. Moreover, [19] uses an external force estimator, without employing force sensors, [4] presents a force sensor-free control protocol with gain tuning, and [11] considers the object regulation problem without force/torque feedback. Finally, force/torque sensor-free methodologies are developed in [25], where the robot dynamics are not taken into account, and in [23], where a linearization technique is employed.

Another important characteristic is the representation of the agent and object orientation. The most commonly used tools for orientation representation consist of rotation matrices, Euler angles, and the angle/axis convention. Rotation matrices, however, are not used very often in robotic manipulation tasks due to the difficulty of extracting an error vector from them. Moreover, the mapping from Euler angle/axis values to angular velocities exhibits singularities at certain points, rendering thus these representations incompetent. On the other hand, the representation using unit quaternions, which is employed in this work, constitutes a singularity-free orientation representation, without complicating the control design. In cooperative manipulation tasks, unit quaternions are employed in [11], [12], [26] as well as [27], where the interaction dynamics of cooperative manipulation are analyzed.

In addition, most works in the related literature consider known dynamic parameters regarding the object and the robotic agents. However, the accurate knowledge of such parameters, such as masses or moments of inertia, can be a challenging issue, especially for complex robotic manipulators; adaptive control protocols are proposed in [5] with a gain tuning scheme, in [11], where the object regulation problem is considered, as well as in [6] and [20]. An estimation of parameters is included in [25], whereas [21] and [22] employ fuzzy mechanisms to compensate model uncertainties. In [24] the authors develop a task-oriented adaptive control protocol using observers. Kinematic uncertainties are handled in [26] and [14].

An internal force and load distribution analysis is performed in [28]; [18] employs a leader-follower scheme, and [29] develops a decentralized force consensus algorithm. Furthermore, [30] introduces hybrid modeling of cooperative manipulation schemes and [31] includes intermittent contact; [32] proposes a kinematic-based multi-robot manipulation scheme,

The authors are with the Centre for Autonomous Systems and ACCESS Linnaeus Centre, KTH Royal Institute of Technology, Stockholm 10044, Sweden. Emails: {cverginis, matteoma, dimos}@kth.se.

This work was supported by the H2020 ERC Starting Grant BUCOPHSYS, the Swedish Research Council (VR), the Knut och Alice Wallenberg Foundation, the European Union's Horizon 2020 Research and Innovation Programme under the Grant Agreement No. 644128 (AEROWORKS), the Swedish Foundation for Strategic Research (SSF), and the EU H2020 Research and Innovation Programme under GA No. 731869 (Co4Robots).

and [33] addresses the problem from a formation-control point of view. Finally, in [34] a navigation function-based approach is used and in our previous work [35] we considered an MPC approach for the centralized cooperative object transportation.

### A. Contribution and Outline

In this paper, we propose two novel nonlinear control protocols for the trajectory tracking by the center of mass of an object that is rigidly grasped by  $N$  robotic agents, without using force/torque measurements at the grasping points.

Firstly, we develop a decentralized control scheme that combines (i) adaptation laws to compensate for external disturbances and uncertainties of the agents' and the object's dynamic parameters, with (ii) quaternion modeling of the object's orientation which avoids undesired representation singularities. A preliminary result on the specific adaptive scheme was developed in [36], whose control law, however, was slightly different and was not tested experimentally or in simulation. Secondly, we propose a decentralized model-free control scheme that guarantees *predefined* transient and steady-state performance for the object's center of mass. We provide detailed stability analysis for both control schemes. Finally, simulation and experimental results with two agents verify the validity of the proposed schemes.

The rest of the paper is organized as follows. Section II provides the notation used throughout the paper and necessary background. The modeling of the system as well as the problem formulation are given in Section III. Section IV presents the details of the two proposed control schemes with the corresponding stability analysis, and Section V illustrates the simulation and experimental results. Finally, Section VI concludes the paper.

## II. NOTATION AND PRELIMINARIES

### A. Notation

The set of positive integers is denoted by  $\mathbb{N}$  and the real  $n$ -coordinate space, with  $n \in \mathbb{N}$ , by  $\mathbb{R}^n$ ;  $\mathbb{R}_{\geq 0}^n$  and  $\mathbb{R}_{>0}^n$  are the sets of real  $n$ -vectors with all elements nonnegative and positive, respectively. The  $n \times n$  identity matrix is denoted by  $I_n$ , the  $n$ -dimensional zero vector by  $0_n$  and the  $n \times m$  matrix with zero entries by  $0_{n \times m}$ . The  $n$ -dimensional vector of ones is denoted by  $\mathbb{1}_n$ . Given a matrix  $A \in \mathbb{R}^{n \times m}$ , we use  $\|A\| := \sqrt{\lambda_{\max}(A^T A)}$ , where  $\lambda_{\max}(\cdot)$  is the maximum eigenvalue of a matrix. The vector connecting the origins of coordinate frames  $\{A\}$  and  $\{B\}$  expressed in frame  $\{C\}$  coordinates in 3-D space is denoted as  $p_{B/A}^C \in \mathbb{R}^3$ . Given  $a \in \mathbb{R}^3$ ,  $S(a)$  is the skew-symmetric matrix defined according to  $S(a)b = a \times b$ . The rotation matrix from  $\{A\}$  to  $\{B\}$  is denoted as  $R_{B/A} \in SO(3)$ , where  $SO(3)$  is the 3-D rotation group. The angular velocity of frame  $\{B\}$  with respect to  $\{A\}$  is denoted as  $\omega_{B/A} \in \mathbb{R}^3$  and it holds that [37]  $\dot{R}_{B/A} = S(\omega_{B/A})R_{B/A}$ . We further denote as  $\eta_{A/B} \in \mathbb{T}$  the Euler angles representing the orientation of  $\{B\}$  with respect to  $\{A\}$ , with  $\mathbb{T} := (-\pi, \pi) \times (-\frac{\pi}{2}, \frac{\pi}{2}) \times (-\pi, \pi)$ . We also define the set  $\mathbb{M} = \mathbb{R}^3 \times \mathbb{T}$ . In addition,  $S^n$  denotes the  $(n+1)$ -dimensional sphere. Given a state  $x$ , with  $\dot{x} = f(x, t)$ , and a function  $g(x, t)$ , (which may represent a state transformation),

the derivative of  $g(x, t)$  is  $\dot{g}(x, t) = \frac{\partial g(x, t)}{\partial x} f(x, t) + \frac{\partial g(x, t)}{\partial t}$ , where  $\frac{\partial g(x, t)}{\partial x}$  has the appropriate dimensions. For notational brevity, when a coordinate frame corresponds to an inertial frame of reference  $\{I\}$ , we will omit its explicit notation (e.g.,  $p_B = p_{B/I}^I, \omega_B = \omega_{B/I}^I, R_B = R_{B/I}$  etc.). Finally, all vector and matrix differentiations will be with respect to an inertial frame  $\{I\}$ , unless otherwise stated.

### B. Unit Quaternions

Given two frames  $\{A\}$  and  $\{B\}$ , we define a unit quaternion  $\zeta_{B/A} := [\varphi_{B/A}, \epsilon_{B/A}^T]^T \in S^3$  describing the orientation of  $\{B\}$  with respect to  $\{A\}$ , with  $\varphi_{B/A} \in \mathbb{R}, \epsilon_{B/A} \in \mathbb{R}^3$ , subject to the constraint  $\varphi_{B/A}^2 + \epsilon_{B/A}^T \epsilon_{B/A} = 1$ . The relation between  $\zeta_{B/A}$  and the corresponding rotation matrix  $R_{B/A}$  as well as the axis/angle representation can be found in [37]. For a given quaternion  $\zeta_{B/A} = [\varphi_{B/A}, \epsilon_{B/A}^T]^T \in S^3$ , its conjugate, that corresponds to the orientation of  $\{A\}$  with respect to  $\{B\}$ , is [37]  $\zeta_{B/A}^+ = [\varphi_{B/A}, -\epsilon_{B/A}^T]^T \in S^3$ . Moreover, given two quaternions  $\zeta_i := \zeta_{B_i/A_i} = [\varphi_{B_i/A_i}, \epsilon_{B_i/A_i}^T]^T, \forall i \in \{1, 2\}$ , the quaternion product is defined as [37]

$$\zeta_1 \otimes \zeta_2 = \begin{bmatrix} \varphi_1 \varphi_2 - \epsilon_1^T \epsilon_2 \\ \varphi_1 \epsilon_2 + \varphi_2 \epsilon_1 + S(\epsilon_1) \epsilon_2 \end{bmatrix} \in S^3, \quad (1)$$

where  $\varphi_i := \varphi_{B_i/A_i}, \epsilon_i := \epsilon_{B_i/A_i}, \forall i \in \{1, 2\}$ .

For a moving frame  $\{B\}$  (with respect to  $\{A\}$ ), the time derivative of the quaternion  $\zeta_{B/A} = [\varphi_{B/A}, \epsilon_{B/A}^T]^T \in S^3$  is given by [37]:

$$\dot{\zeta}_{B/A} = \frac{1}{2} E(\zeta_{B/A}) \omega_{B/A}^A, \quad (2a)$$

where  $E : S^3 \rightarrow \mathbb{R}^{4 \times 3}$  is defined as:

$$E(\zeta) = \begin{bmatrix} -\epsilon^T \\ \varphi I_3 - S(\epsilon) \end{bmatrix}, \forall \zeta = [\varphi, \epsilon^T]^T \in S^3.$$

Finally, it can be shown that  $[E(\zeta)]^T E(\zeta) = I_3, \forall \zeta \in S^3$  and hence (2a) implies

$$\omega_{B/A}^A = 2[E(\zeta_{B/A})]^T \dot{\zeta}_{B/A}. \quad (2b)$$

It can be also shown that

$$\dot{\omega}_{B/A}^A = 2[E(\zeta_{B/A})]^T \ddot{\zeta}_{B/A}. \quad (2c)$$

### C. Prescribed Performance

Prescribed performance control, recently proposed in [38], describes the behavior where a tracking error  $e : \mathbb{R}_{\geq 0} \rightarrow \mathbb{R}$  evolves strictly within a predefined region that is bounded by certain functions of time, achieving prescribed transient and steady state performance. The mathematical expression of prescribed performance is given by the following inequalities:

$$-\rho_L(t) < e(t) < \rho_U(t), \quad \forall t \in \mathbb{R}_{\geq 0},$$

where  $\rho_L(t), \rho_U(t)$  are smooth and bounded decaying functions of time satisfying  $\lim_{t \rightarrow \infty} \rho_L(t) > 0$  and  $\lim_{t \rightarrow \infty} \rho_U(t) > 0$ , called performance functions. Specifically, for the exponential performance functions  $\rho_i(t) := (\rho_{i,0} - \rho_{i,\infty}) \exp(-l_i t) + \rho_{i,\infty}$ , with  $\rho_{i,0}, \rho_{i,\infty}, l_i \in \mathbb{R}_{>0}, i \in \{U, L\}$ , appropriately chosen constants, the terms  $\rho_{L,0} := \rho_L(0), \rho_{U,0} := \rho_U(0)$  are

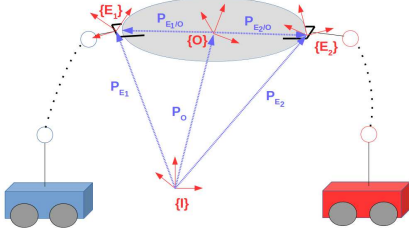


Fig. 1: Two robotic agents rigidly grasping an object.

selected such that  $\rho_{U,0} > e(0) > \rho_{L,0}$  and the terms  $\rho_{L,\infty} := \lim_{t \rightarrow \infty} \rho_L(t)$ ,  $\rho_{U,\infty} := \lim_{t \rightarrow \infty} \rho_U(t)$  represent the maximum allowable size of the tracking error  $e(t)$  at steady state, which may be set arbitrarily small to a value reflecting the resolution of the measurement device, thus achieving practical convergence of  $e(t)$  to zero. Moreover, the decreasing rate of  $\rho_L(t)$ ,  $\rho_U(t)$ , which is affected by the constants  $l_L, l_U$  in this case, introduces a lower bound on the required speed of convergence of  $e(t)$ . Therefore, the appropriate selection of the performance functions  $\rho_L(t)$ ,  $\rho_U(t)$  imposes performance characteristics on the tracking error  $e(t)$ .

#### D. Dynamical Systems

Consider the initial value problem:

$$\dot{\sigma} = H(\sigma, t), \sigma(0) \in \Omega, \quad (3)$$

with  $H : \Omega \times \mathbb{R}_{\geq 0} \rightarrow \mathbb{R}^n$  where  $\Omega \subset \mathbb{R}^n$  is a non-empty open set.

**Definition 1.** [39] A solution  $\sigma(t)$  of the initial value problem (3) is maximal if it has no proper right extension that is also a solution of (3).

**Theorem 1.** [39] Consider problem (3). Assume that  $H(\sigma, t)$  is: a) locally Lipschitz on  $\sigma$  for almost all  $t \in \mathbb{R}_{\geq 0}$ , b) piecewise continuous on  $t$  for each fixed  $\sigma \in \Omega$  and c) locally integrable on  $t$  for each fixed  $\sigma \in \Omega$ . Then, there exists a maximal solution  $\sigma(t)$  of (3) on  $[0, t_{\max})$  with  $t_{\max} > 0$  such that  $\sigma(t) \in \Omega, \forall t \in [0, t_{\max})$ .

**Proposition 1.** [39] Assume that the hypotheses of Theorem 1 hold. For a maximal solution  $\sigma(t)$  on the time interval  $[0, t_{\max})$  with  $t_{\max} < \infty$  and for any compact set  $\Omega' \subset \Omega$  there exists a time instant  $t' \in [0, t_{\max})$  such that  $\sigma(t') \notin \Omega'$ .

### III. PROBLEM FORMULATION

Consider  $N$  fully actuated robotic agents rigidly grasping an object (see Fig. 1). We denote by  $\{E_i\}$ ,  $\{O\}$  the end-effector and object's center of mass frames, respectively;  $\{I\}$  corresponds to an inertial frame of reference, as mentioned in Section II-A. The rigidity assumption implies that the agents can exert both forces and torques along all directions to the object. In the following, we present the modeling of the coupled kinematics and dynamics of the object and the agents.

#### A. Robotic Agents

We denote by  $q_i, \dot{q}_i \in \mathbb{R}^{n_i}$ , with  $n_i \in \mathbb{N}, \forall i \in \mathcal{N}$ , the generalized joint-space variables and their time derivatives of agent  $i$ , with  $q_i := [q_{i1}, \dots, q_{in_i}]$ . The overall joint configuration is then  $q := [q_1^\top, \dots, q_N^\top]^\top, \dot{q} := [\dot{q}_1^\top, \dots, \dot{q}_N^\top]^\top \in \mathbb{R}^n$ , with  $n := \sum_{i \in \mathcal{N}} n_i$ . In addition, the inertial position and Euler-angle orientation of the  $i$ th end-effector, denoted by  $p_{E_i}$  and  $\eta_{E_i}$ , respectively, can be derived by the forward kinematics and are smooth functions of  $q_i$ , i.e.  $p_{E_i} : \mathbb{R}^{n_i} \rightarrow \mathbb{R}^3$ ,  $\eta_{E_i} : \mathbb{R}^{n_i} \rightarrow \mathbb{T}$ . The differential equation describing the dynamics of each agent is [37]:

$$B_i(q_i)\ddot{q}_i + C_{q_i}(q_i, \dot{q}_i)\dot{q}_i + g_{q_i}(q_i) + d_{q_i}(q_i, \dot{q}_i, t) = \tau_i - [J_i(q_i)]^\top f_i, \quad (4)$$

where  $B_i : \mathbb{R}^{n_i} \rightarrow \mathbb{R}^{n_i \times n_i}$  is the positive definite inertia matrix,  $C_{q_i} : \mathbb{R}^{2n_i} \rightarrow \mathbb{R}^{n_i \times n_i}$  is the Coriolis matrix,  $g_{q_i} : \mathbb{R}^{n_i} \rightarrow \mathbb{R}^{n_i}$  is the joint-space gravity term,  $d_{q_i} : \mathbb{R}^{2n_i} \times \mathbb{R}_{\geq 0} \rightarrow \mathbb{R}^{n_i}$  is a bounded vector representing unmodeled friction, uncertainties and external disturbances,  $f_i \in \mathbb{R}^6$  is the vector of generalized forces that agent  $i$  exerts on the grasping point with the object and  $\tau_i \in \mathbb{R}^{n_i}$  is the vector of joint torques, acting as control inputs  $\forall i \in \mathcal{N}$ .

The generalized velocity of each agent's end-effector  $v_i := [\dot{p}_{E_i}^\top, \omega_{E_i}^\top]^\top \in \mathbb{R}^6$ , can be considered as a transformed state through the differential kinematics  $v_i = J_i(q_i)\dot{q}_i$  [37], where  $J_i : \mathbb{R}^{n_i} \rightarrow \mathbb{R}^{6 \times n_i}$  is a smooth function representing the geometric Jacobian matrix,  $\forall i \in \mathcal{N}$  [37]. The latter leads also to

$$\dot{v}_i = J_i(q_i)\ddot{q}_i + J_i^d(q_i, \dot{q}_i)\dot{q}_i, \quad (5)$$

where  $J_i^d : \mathbb{R}^{2n_i} \rightarrow \mathbb{R}^{6 \times n_i}$  represents the Jacobian derivative function, with  $J_i^d(q_i, \dot{q}_i) := \dot{J}_i(q_i)$ . Then, by employing the differential kinematics as well as (5), we obtain from (4) the transformed task space dynamics [37]:

$$M_i(q_i)\dot{v}_i + C_i(q_i, \dot{q}_i)v_i + g_i(q_i) + d_i(q_i, \dot{q}_i, t) = u_i - f_i, \quad (6)$$

with the corresponding task space terms  $M_i : \mathbb{R}^{n_i} \rightarrow \mathbb{R}^{6 \times 6}$ ,  $C_i : \mathbb{R}^{2n_i} \rightarrow \mathbb{R}^{6 \times 6}$ ,  $g_i : \mathbb{R}^{n_i} \rightarrow \mathbb{R}^6$ ,  $d_i : \mathbb{R}^{2n_i} \times \mathbb{R}_{\geq 0} \rightarrow \mathbb{R}^6$  and  $u_i \in \mathbb{R}^6$  being the task space wrench, related to  $\tau_i$  via  $\tau_i = J_i^\top(q_i)u_i + (I_{n_i} - J_i^\top(q_i)\tilde{J}_i^\top(q_i))\tau_{i0}$ , where  $\tilde{J}_i$  is a generalized inverse of  $J_i$  [37];  $\tau_{i0}$  concerns redundant agents ( $n_i > 6$ ) and does not contribute to end-effector forces.

The agent task-space dynamics (6) can be written in vector form as:

$$M(q)\dot{v} + C(q, \dot{q})v + g(q) + d(q, \dot{q}, t) = u - f, \quad (7)$$

where  $v := [v_1^\top, \dots, v_N^\top]^\top \in \mathbb{R}^{6N}$ ,  $M := \text{diag}\{[M_i]_{i \in \mathcal{N}}\} \in \mathbb{R}^{6N \times 6N}$ ,  $C := \text{diag}\{[C_i]_{i \in \mathcal{N}}\} \in \mathbb{R}^{6N \times 6N}$ ,  $f := [f_1^\top, \dots, f_N^\top]^\top$ ,  $u := [u_1^\top, \dots, u_N^\top]^\top$ ,  $g := [g_1^\top, \dots, g_N^\top]^\top$ ,  $d := [d_1^\top, \dots, d_N^\top]^\top \in \mathbb{R}^{6N}$ .

#### B. Object

Regarding the object, we denote by  $x_o := [p_o^\top, \eta_o^\top]^\top \in \mathbb{M}$ ,  $v_o := [\dot{p}_o^\top, \dot{\eta}_o^\top]^\top \in \mathbb{R}^{12}$  the pose and generalized velocity of the object's center of mass, which is considered as the object's

state. We consider the following second order dynamics, which can be derived based on the Newton-Euler formulation:

$$\dot{x}_o = J_o(\eta_o)v_o, \quad (8a)$$

$$M_o(x_o)\dot{v}_o + C_o(x_o, \dot{x}_o)v_o + g_o(x_o) + d_o(x_o, \dot{x}_o, t) = f_o, \quad (8b)$$

where  $M_o : \mathbb{M} \rightarrow \mathbb{R}^{6 \times 6}$  is the positive definite inertia matrix,  $C_o : \mathbb{M} \times \mathbb{R}^6 \rightarrow \mathbb{R}^{6 \times 6}$  is the Coriolis matrix,  $g_o : \mathbb{M} \rightarrow \mathbb{R}^6$  is the gravity vector,  $d_o : \mathbb{M} \times \mathbb{R}^6 \times \mathbb{R}_{\geq 0} \rightarrow \mathbb{R}^6$  a bounded vector representing modeling uncertainties and external disturbances, and  $f_o \in \mathbb{R}^6$  is the vector of generalized forces acting on the object's center of mass. Moreover,  $J_o : \mathbb{T} \rightarrow \mathbb{R}^{6 \times 6}$  is the object representation Jacobian  $J_o(\eta_o) := \text{diag}\{I_3, J_{o_\eta}(\eta_o)\}$ , where  $J_{o_\eta} : \mathbb{T} \rightarrow \mathbb{R}^{3 \times 3}$ :

$$J_{o_\eta}(\eta_o) := \begin{bmatrix} 1 & \sin(\phi_o) \tan(\theta_o) & \cos(\phi_o) \tan(\theta_o) \\ 0 & \cos(\phi_o) & -\sin(\theta_o) \\ 0 & \frac{\sin(\phi_o)}{\cos(\theta_o)} & \frac{\cos(\phi_o)}{\cos(\theta_o)} \end{bmatrix},$$

and is not well-defined when  $\theta_o = \pm \frac{\pi}{2}$ , which is referred to as *representation singularity*. Moreover, it can be proved that

$$\|J_o(\eta_o)\| = \sqrt{\frac{|\sin(\theta_o)|+1}{1-\sin^2(\theta_o)}}, \quad (9)$$

which will be used in the subsequent analysis.

A possible way to avoid the aforementioned singularity is to transform the Euler angles to a unit quaternion representation for the orientation. Hence, the term  $\eta_o$  can be transformed to the unit quaternion  $\zeta_o = [\varphi_o, \epsilon_o^\top]^\top \in S^3$  [37], for which, following Section II-B and (2), one obtains:

$$\begin{aligned} \dot{\zeta}_o &= \frac{1}{2}E(\zeta_o)\omega_o \\ \omega_o &= 2[E(\zeta_o)]^\top \dot{\zeta}_o, \end{aligned}$$

which is a singularity-free representation.

### C. Coupled Dynamics

In view of Fig. 1, one concludes that the pose of the agents and the object's center of mass are related as

$$p_{E_i}(q_i) = p_o + p_{E_i/o}(q_i) = p_o + R_{E_i}(q_i)p_{E_i/o}^{E_i}, \quad (10a)$$

$$\eta_{E_i}(q_i) = \eta_o + \eta_{E_i/o}, \quad (10b)$$

$\forall i \in \mathcal{N}$ , where  $p_{E_i/o}^{E_i}$  and  $\eta_{E_i/o}$  are the *constant* distance and orientation offset between  $\{O\}$  and  $\{E_i\}$ . Following (10), along with the fact that, due to the grasping rigidity, it holds that  $\omega_{E_i} = \omega_o, \forall i \in \mathcal{N}$ , one obtains

$$v_i = J_{o_i}(q_i)v_o, \quad (11)$$

where  $J_{o_i} : \mathbb{R}^{n_i} \rightarrow \mathbb{R}^{6 \times 6}$  is the object-to-agent Jacobian matrix, with

$$J_{o_i}(x) = \begin{bmatrix} I_3 & S(p_{o/E_i}(x)) \\ 0_{3 \times 3} & I_3 \end{bmatrix}, \forall x \in \mathbb{R}^{n_i}, \quad (12)$$

which is always full-rank. Moreover, from (11), one obtains

$$\dot{v}_i = J_{o_i}(q_i)\dot{v}_o + J_{o_i}^d(q_i, \dot{q}_i)v_o \quad (13)$$

and  $J_{o_i}^d : \mathbb{R}^{2n_i} \rightarrow \mathbb{R}^{6 \times 6}$ , with  $J_{o_i}^d(q_i, \dot{q}_i) := \dot{J}_{o_i}(q_i)$ . In addition, it can be proved for  $J_{o_i}$  that

$$\|J_{o_i}(x)\| \leq \|p_{o/E_i}^{E_i}\| + 1, \forall x \in \mathbb{R}^{n_i}, i \in \mathcal{N}, \quad (14)$$

which will be used in the subsequent analysis.

The kineto-statics duality along with the grasp rigidity suggest that the force  $f_o$  acting on the object's center of mass and the generalized forces  $f_i, i \in \mathcal{N}$ , exerted by the agents at the grasping points, are related through:

$$f_o = [G(q)]^\top f, \quad (15)$$

where  $G : \mathbb{R}^n \rightarrow \mathbb{R}^{6N \times 6}$ , with  $G(q) := [[J_{o_1}(q_1)]^\top, \dots, [J_{o_N}(q_N)]^\top]^\top$ , is the full column-rank grasp matrix. By substituting (7) into (15), we obtain:

$$f_o = [G(q)]^\top (u - M(q)\dot{v} - C(q, \dot{q})v - g(q) - d(q, \dot{q}, t)),$$

which, after substituting (11), (13), (8), and rearranging terms, yields the overall system coupled dynamics:

$$\tilde{M}(x)\dot{v}_o + \tilde{C}(x)v_o + \tilde{g}(x) + \tilde{d}(x, t) = [G(q)]^\top u, \quad (16)$$

where

$$\tilde{M}(x) := M_o(x_o) + [G(q)]^\top M(q)G(q) \quad (17a)$$

$$\begin{aligned} \tilde{C}(x) &:= C_o(x_o, \dot{x}_o) + [G(q)]^\top C(q, \dot{q})G(q) \\ &\quad + [G(q)]^\top M(q)G^d(q, \dot{q}) \end{aligned} \quad (17b)$$

$$\tilde{g}(x) := g_o(x_o) + [G(q)]^\top g(q). \quad (17c)$$

$$\tilde{d}(x, t) := d_o(x_o, \dot{x}_o, t) + [G(q)]^\top d(q, \dot{q}, t) \quad (17d)$$

$$G^d(q, \dot{q}) := [[J_{o_1}^d(q_1, \dot{q}_1)]^\top, \dots, [J_{o_N}^d(q_N, \dot{q}_N)]^\top]^\top, \quad (17e)$$

and  $x$  is the overall state  $x := [q^\top, \dot{q}^\top, x_o^\top, \dot{x}_o^\top]^\top \in \mathbb{R}^{2n+6} \times \mathbb{M}$ . Moreover, the following Lemma is necessary for the following analysis.

**Lemma 1.** *The matrix  $\tilde{M}(x)$  is symmetric and positive definite and the matrix  $\dot{\tilde{M}}(x) - 2\tilde{C}(x)$  is skew symmetric, i.e.,*

$$[\dot{\tilde{M}}(x) - 2\tilde{C}(x)]^\top = -[\dot{\tilde{M}}(x) - 2\tilde{C}(x)], \forall x \in \mathbb{R}^6$$

$$y^\top [\dot{\tilde{M}}(x) - 2\tilde{C}(x)] y = 0, \quad \forall x, y \in \mathbb{R}^6.$$

*Proof:* The matrices  $M_o$  and  $M_i$  are symmetric and positive definite,  $\forall i \in \mathcal{N}$  and the matrices  $\dot{M}_i(q_i) - 2C_i(q_i, \dot{q}_i)$ ,  $M_o(x_o) - 2C_o(x_o, \dot{x}_o)$  are skew-symmetric,  $\forall i \in \mathcal{N}$  [37], which leads to the skew-symmetry of  $\dot{M}(q) - 2C(q, \dot{q})$ . Therefore, since  $G(q)$  is full column-rank, we can conclude the symmetry and positive definiteness of  $\tilde{M}(x)$ . Regarding the skew symmetry of  $\dot{\tilde{M}}(x) - 2\tilde{C}(x)$ , we define first  $A(x) := [\dot{G}(q)]^\top M(q)G(q)$ , and we have from (17b):

$$\begin{aligned} \dot{\tilde{M}}(x) - 2\tilde{C}(x) &= \dot{M}_o(x_o) - 2C_o(x_o, \dot{x}_o) \\ &\quad + [G(q)]^\top (\dot{M}(q) - 2C(q, \dot{q}))G(q) + A(x) - [A(x)]^\top, \end{aligned}$$

which, by employing the skew-symmetry of  $M_o(x_o) - 2C_o(x_o, \dot{x}_o)$  and  $\dot{M}(q) - 2C(q, \dot{q})$ , leads to  $[\dot{\tilde{M}}(x) - 2\tilde{C}(x)]^\top = -[\dot{\tilde{M}}(x) - 2\tilde{C}(x)]$ , which completes the proof. ■



The positive definiteness of  $\widetilde{M}(x)$  leads to the property

$$\underline{m}I_6 \leq \widetilde{M}(x) \leq \bar{m}I_6, \quad (18)$$

$\forall x \in \mathbb{R}^{2n+6} \times \mathbb{R}$ , where  $\underline{m}$  and  $\bar{m}$  are positive unknown constants.

We are now ready to state the problem treated in this paper:

**Problem 1.** *Given a desired bounded object smooth pose trajectory specified by  $\bar{x}_d(t) := [(p_d(t))^\top, (\eta_d(t))^\top]^\top$ ,  $p_d(t) \in \mathbb{R}^3$ ,  $\eta_d(t) := [\varphi_d(t), \theta_d(t), \psi_d(t)] \in \mathbb{T}$ , with bounded first and second derivatives, and  $\theta_d(t) \in [-\bar{\theta}, \bar{\theta}] \subset (-\frac{\pi}{2}, \frac{\pi}{2})$ ,  $\forall t \in \mathbb{R}_{\geq 0}$ , as well as  $v_o(0) = 0_6$ , determine a continuous time-varying control law  $u$  in (16) such that*

$$\lim_{t \rightarrow \infty} \begin{bmatrix} p_o(t) \\ \eta_o(t) \end{bmatrix} = \begin{bmatrix} p_d(t) \\ \eta_d(t) \end{bmatrix}.$$

The requirement  $\theta_d(t) \in [-\bar{\theta}, \bar{\theta}] \subset (-\frac{\pi}{2}, \frac{\pi}{2})$ ,  $\forall t \in \mathbb{R}_{\geq 0}$  is a necessary condition needed to ensure that tracking of  $\theta_d$  will not result in singular configurations of  $J_o(\eta_o)$ , which is needed for the control protocol of Section IV-B. The constant  $\bar{\theta} \in [0, \frac{\pi}{2})$  can be taken arbitrarily close to  $\frac{\pi}{2}$ .

To solve the aforementioned problem, we need the following assumptions regarding the agent feedback, the bounds of the uncertainties/disturbances, and the kinematic singularities.

**Assumption 1. (Feedback)** *Each agent  $i \in \mathcal{N}$  has continuous feedback of its own state  $q_i, \dot{q}_i$ .*

**Assumption 2. (Object Geometry)** *Each agent  $i \in \mathcal{N}$  knows the constant offsets  $p_{E_i/O}^{E_i}$  and  $\eta_{E_i/O}$ ,  $\forall i \in \mathcal{N}$ .*

**Assumption 3. (Kinematic Singularities)** *The robotic agents operate away from kinematic singularities, i.e.,  $q_i \in \{q_i \in \mathbb{R}^{n_i} : |\det(J_i(q_i)[J_i(q_i)]^\top)| \geq \underline{J}_i > 0\}$  for positive constants  $\underline{J}_i > 0$ ,  $\forall i \in \mathcal{N}$ .*

Assumption 1 is realistic for real manipulation systems, since on-board sensor can provide accurately the measurements  $q_i, \dot{q}_i$ . The object geometrical characteristics in Assumption 2 can be obtained by on-board sensors, whose inaccuracies are not modeled here and constitute part of future work. Finally, Assumption 3, although it does not hold for any  $q_i \in \mathbb{R}^{n_i}$ , will be used only for those  $q_i$  that bring  $x_o$  close to the desired trajectory  $\bar{x}_d(t)$ . Intuitively, this assumption states that the  $q_i$  that achieve  $x_o(t) = \bar{x}_d(t)$ ,  $\forall t \in \mathbb{R}_{\geq 0}$  are sufficiently far from singular configurations.

Since each agent has feedback from its state  $q_i, \dot{q}_i$ , it can compute through the forward and differential kinematics the end-effector pose  $p_{E_i}(q_i), \eta_{E_i}(q_i)$  and the velocity  $v_i$ ,  $\forall i \in \mathcal{N}$ . Moreover, since it knows  $p_{E_i/O}^{E_i}$  and  $\eta_{E_i/O}$ , it can compute  $J_{o_i}(q_i)$  from (12), and  $x_o, v_o$  by inverting (10) and (11), respectively. Consequently, each agent can then compute the object unit quaternion  $\zeta_o$  as well as  $\dot{\zeta}_o$ .

#### IV. MAIN RESULTS

In this section we present two control schemes for the solution of Problem 1. The proposed controllers are decentralized, in the sense that the agents calculate their control signal on their own, without communicating with each other, as well

as robust, since they do not take into account the dynamic properties of the agents or the object (mass/inertia moments) or the uncertainties/external disturbances modeled by the function  $\widetilde{d}(x, t)$  in (16). The first control scheme is presented in Section IV-A, and is based on quaternion feedback and adaptation laws, while the second control scheme is given in Section IV-B and is inspired by the Prescribed Performance Control (PPC) Methodology introduced in [38].

##### A. Adaptive Control with Quaternion Feedback

Firstly, we need the following assumption regarding the model uncertainties/external disturbances.

**Assumption 4. (Uncertainties/Disturbance parameterization)** *There exists positive, finite unknown constants  $\bar{d}_o, \bar{d}_i$  and known bounded functions  $\delta_o : \mathbb{M} \times \mathbb{R}^6 \times \mathbb{R}_{\geq 0} \rightarrow \mathbb{R}^6, \delta_i : \mathbb{R}^{2n_i} \times \mathbb{R}_{\geq 0} \rightarrow \mathbb{R}^6$ , such that*

$$\begin{aligned} d_o(x_o, \dot{x}_o, t) &= \bar{d}_o \delta_o(x_o, \dot{x}_o, t), \\ d_i(q_i, \dot{q}_i, t) &= \bar{d}_i \delta_i(q_i, \dot{q}_i, t), \end{aligned}$$

$$\forall q_i, \dot{q}_i \in \mathbb{R}^{n_i}, x_o \in \mathbb{M}, \dot{x}_o \in \mathbb{R}^6, t \in \mathbb{R}_{\geq 0}, i \in \mathcal{N}.$$

The desired Euler angle orientation vector  $\eta_d : \mathbb{R}_{\geq 0} \rightarrow \mathbb{T}$  is transformed first to the unit quaternion  $\zeta_d : \mathbb{R}_{\geq 0} \rightarrow S^3$  [37]. Then, we need to define the errors associated with the object pose and the desired pose trajectory. We first define the state that corresponds to the position error:

$$e_p := p_o - p_d(t).$$

Since unit quaternions do not form a vector space, they cannot be subtracted to form an orientation error; instead we should use the properties of the quaternion group algebra. Let  $e_\zeta = [e_\varphi, e_\epsilon]^\top \in S^3$  be the unit quaternion describing the orientation error. Then, it holds that [37],

$$e_\zeta = \zeta_d(t) \otimes \zeta_o^+ = \begin{bmatrix} \varphi_d(t) \\ \epsilon_d(t) \end{bmatrix} \otimes \begin{bmatrix} \varphi_o \\ -\epsilon_o \end{bmatrix},$$

which, by using (1), becomes:

$$e_\zeta = \begin{bmatrix} e_\varphi \\ e_\epsilon \end{bmatrix} := \begin{bmatrix} \varphi_o \varphi_d(t) + \epsilon_o^\top \epsilon_d(t) \\ \varphi_o \epsilon_d(t) - \varphi_d(t) \epsilon_o + S(\epsilon_o) \epsilon_d(t) \end{bmatrix}. \quad (19)$$

By employing (2) and certain properties of skew-symmetric matrices [40], it can be shown that the error dynamics of  $e_p, e_\varphi$  are:

$$\dot{e}_p = \dot{p}_o - \dot{p}_d(t) \quad (20a)$$

$$\dot{e}_\varphi = \frac{1}{2} e_\epsilon^\top e_\omega \quad (20b)$$

$$\dot{e}_\epsilon = -\frac{1}{2} [e_\varphi I_3 + S(e_\epsilon)] e_\omega - S(e_\epsilon) \omega_d(t), \quad (20c)$$

where  $e_\omega := \omega_o - \omega_d(t)$  is a state for the angular velocity error, with  $\omega_d(t) = 2[E(\zeta_d(t))]^\top \dot{\zeta}_d(t)$ , as indicated by (2b).

Due to the ambiguity of unit quaternions, when  $\zeta_o = \zeta_d$ , then  $e_\zeta = [1, 0_3^\top]^\top \in S^3$ . If  $\zeta_o = -\zeta_d$ , then  $e_\zeta = [-1, 0_3^\top]^\top \in S^3$ , which, however, represents the same orientation. Therefore, the control objective established in Problem 1 is equivalent to

$$\lim_{t \rightarrow \infty} \begin{bmatrix} e_p(t) \\ |e_\varphi(t)| \\ e_\epsilon(t) \end{bmatrix} = \begin{bmatrix} 0_3 \\ 1 \\ 0_3 \end{bmatrix}.$$

The left hand side of (6), after employing (11) and (13), becomes

$$\begin{aligned} & M_i(q_i)\dot{v}_i + C_i(q_i, \dot{q}_i)v_i + g_i(q_i) + d_i(q_i, \dot{q}_i, t) = \\ & M_i(q_i)\left(J_{O_i}(q_i)\dot{v}_O + J_{O_i}^d(q_i, \dot{q}_i)v_O\right) + C_i(q_i, \dot{q}_i)J_{O_i}(q_i)v_O + \\ & g_i(q_i) + d_i(q_i, \dot{q}_i, t). \end{aligned}$$

which, according to Assumption 4 and the fact that the manipulator dynamics can be linearly parameterized with respect to dynamic parameters [41], becomes

$$\begin{aligned} & M_i(q_i)J_{O_i}(q_i)\dot{v}_O + \left(M_i(q_i)J_{O_i}^d(q_i, \dot{q}_i) + C_i(q_i, \dot{q}_i)J_{O_i}(q_i)\right)v_O \\ & + g_i(q_i) + d_i(q_i, \dot{q}_i, t) = H_i(q_i, \dot{q}_i, v_O, \dot{v}_O)\vartheta_i + \bar{d}_i\delta_i(q_i, \dot{q}_i, t), \end{aligned} \quad (21a)$$

$\forall i \in \mathcal{N}$ , where  $\vartheta_i \in \mathbb{R}^\ell$ ,  $\ell \in \mathbb{N}$ , are vectors of unknown but constant dynamic parameters of the agents, appearing in the terms  $M_i$ ,  $C_i$ ,  $g_i$ , and  $H_i : \mathbb{R}^{2n_i+12} \rightarrow \mathbb{R}^{6 \times \ell}$  are known regressor matrices, independent of  $\vartheta_i$ ,  $i \in \mathcal{N}$ . Without loss of generality, we assume here that the dimension of  $\vartheta_i$  is the same,  $\ell$  for all the agents. Similarly, the dynamical terms of the left hand side of (8b) can be written as

$$\begin{aligned} & M_O(x_O)\dot{v}_O + C_O(x_O, \dot{x}_O)v_O + g_O(x_O) + d_O(x_O, \dot{x}_O, t) \\ & = Y_O(x_O, \dot{x}_O, v_O, \dot{v}_O)\vartheta_O + \bar{d}_O\delta_O(x_O, \dot{x}_O, t), \end{aligned} \quad (21b)$$

where  $\vartheta_O \in \mathbb{R}^{\ell_O}$ ,  $\ell_O \in \mathbb{N}$  is a vector of unknown but constant dynamic parameters of the object, appearing in the terms  $M_O$ ,  $C_O$ ,  $g_O$ , and  $Y_O : \mathbb{M} \times \mathbb{R}^{18} \rightarrow \mathbb{R}^{6 \times \ell_O}$  is a known regressor matrices, independent of  $\vartheta_O$ . It is worth noting that the choice for  $\ell$  and  $\ell_O$  is not unique. In the same vein, since  $J_{O_i}(q_i)$ , as given in (12), depends only on  $q_i$  and not on  $\vartheta_i$ ,  $\vartheta_O$ ,  $\forall i \in \mathcal{N}$ , we can write:

$$\begin{aligned} & [J_{O_i}(q_i)]^\top M_i(q_i)J_{O_i}(q_i)\dot{v}_O + [J_{O_i}(q_i)]^\top g_i(q_i) + \\ & \left([J_{O_i}(q_i)]^\top M_i(q_i)J_{O_i}^d(q_i, \dot{q}_i) + [J_{O_i}(q_i)]^\top C_i(q_i, \dot{q}_i)J_{O_i}(q_i)\right)v_O \\ & + [J_{O_i}(q_i)]^\top d_i(q_i, \dot{q}_i, t) = Y_i(q_i, \dot{q}_i, v_O, \dot{v}_O)\vartheta_i \\ & + [J_{O_i}(q_i)]^\top \bar{d}_i\delta_i(q_i, \dot{q}_i, t), \end{aligned} \quad (22)$$

where  $Y_i : \mathbb{R}^{2n_i+12} \rightarrow \mathbb{R}^{6 \times \ell}$  are also regressor matrices independent of  $\vartheta_i$ ,  $\vartheta_O$ . Hence, in view of (17), (21) and (22), the left-hand side of (16) can be written as:

$$\begin{aligned} & \widetilde{M}(x)\dot{v}_O + \widetilde{C}(x)v_O + \widetilde{g}(x) + \widetilde{d}(x, t) = Y_O(x_O, \dot{x}_O, v_O, \dot{v}_O)\vartheta_O \\ & + [Y(q, \dot{q}, v_O, \dot{v}_O)]^\top \vartheta + \bar{d}_O\delta_O(x_O, \dot{x}_O) + \\ & \sum_{i \in \mathcal{N}} [J_{O_i}(q_i)]^\top \bar{d}_i\delta_i(q_i, \dot{q}_i, t) \end{aligned} \quad (23)$$

where  $\vartheta := [\vartheta_1^\top, \dots, \vartheta_N^\top]^\top \in \mathbb{R}^{N\ell}$  and  $Y(q, \dot{q}, v_O, \dot{v}_O) := [[Y_1(q_1, \dot{q}_1, v_O, \dot{v}_O)]^\top, \dots, [Y_N(q_N, \dot{q}_N, v_O, \dot{v}_O)]^\top]^\top \in \mathbb{R}^{N\ell \times 6}$ .

Let us now introduce the states  $\hat{\vartheta}_{O_i} \in \mathbb{R}^{\ell_O}$  and  $\hat{\vartheta}_i \in \mathbb{R}^\ell$  which represent the estimates of  $\vartheta_O$  and  $\vartheta_i$ , respectively, by agent  $i \in \mathcal{N}$ , and the corresponding stack vectors  $\hat{\vartheta}_O := [(\hat{\vartheta}_{O_1})^\top, \dots, (\hat{\vartheta}_{O_N})^\top]^\top \in \mathbb{R}^{N\ell_O}$ ,  $\hat{\vartheta} := [\hat{\vartheta}_1^\top, \dots, \hat{\vartheta}_N^\top]^\top \in$

$\mathbb{R}^{N\ell}$ , for which we formulate the associated errors  $e_{\vartheta_O} \in \mathbb{R}^{N\ell_O}$ ,  $e_{\vartheta} \in \mathbb{R}^{N\ell}$  as

$$e_{\vartheta_O} := \begin{bmatrix} e_{\vartheta_{O,1}} \\ \vdots \\ e_{\vartheta_{O,N}} \end{bmatrix} := \begin{bmatrix} \vartheta_O - \hat{\vartheta}_{O_1} \\ \vdots \\ \vartheta_O - \hat{\vartheta}_{O_N} \end{bmatrix} = \vartheta_O \cdot \mathbb{1}_{N\ell_O} - \hat{\vartheta}_O \quad (24a)$$

$$e_{\vartheta} := \begin{bmatrix} e_{\vartheta_1} \\ \vdots \\ e_{\vartheta_N} \end{bmatrix} := \begin{bmatrix} \vartheta_1 - \hat{\vartheta}_1 \\ \vdots \\ \vartheta_N - \hat{\vartheta}_N \end{bmatrix} = \vartheta - \hat{\vartheta}. \quad (24b)$$

In the same vein, we introduce the states  $\hat{d}_{O_i} \in \mathbb{R}$  and  $\hat{d}_i \in \mathbb{R}$  that correspond to the estimates of the constants  $\bar{d}_O$  and  $\bar{d}_i$ , respectively, by agent  $i \in \mathcal{N}$ , and the corresponding stack vectors  $\bar{d}_O := [\bar{d}_{O_1}, \dots, \bar{d}_{O_N}]^\top \in \mathbb{R}^N$ ,  $\bar{d} := [\bar{d}_1, \dots, \bar{d}_N]^\top \in \mathbb{R}^N$ , for which we also formulate the associated errors  $e_{d_O}, e_d \in \mathbb{R}^N$  as

$$e_{d_O} := \begin{bmatrix} e_{d_{O,1}} \\ \vdots \\ e_{d_{O,2}} \end{bmatrix} := \begin{bmatrix} \bar{d}_O - \hat{d}_{O_1} \\ \vdots \\ \bar{d}_O - \hat{d}_{O_N} \end{bmatrix} = \bar{d}_O \cdot \mathbb{1}_N - \hat{d}_O \quad (25a)$$

$$e_d := \begin{bmatrix} e_{d_1} \\ \vdots \\ e_{d_N} \end{bmatrix} := \begin{bmatrix} \bar{d}_1 - \hat{d}_1 \\ \vdots \\ \bar{d}_N - \hat{d}_N \end{bmatrix} = \bar{d} - \hat{d}, \quad (25b)$$

where we have also used the notation  $\bar{d} := [\bar{d}_1, \dots, \bar{d}_N]^\top$ .

Next, we design the reference velocity  $v_f : \mathbb{R}^6 \times \mathbb{R}_{\geq 0} \rightarrow \mathbb{R}^6$  as

$$v_f(e, t) := v_d(t) - K_f e = \begin{bmatrix} \dot{p}_d(t) - k_p e_p \\ \dot{\omega}_d(t) + k_\zeta e_\zeta \end{bmatrix} \quad (26)$$

with  $K_f := \text{diag}\{k_p, k_\zeta\}$ ,  $e := [e_p^\top, -e_\zeta^\top]^\top \in \mathbb{R}^6$ ,  $k_p, k_\zeta$  positive control gains, and the derivative  $v_f^d : \mathbb{R}^6 \times S^3 \times \mathbb{R}_{\geq 0} \rightarrow \mathbb{R}^6$ , with

$$v_f^d(\dot{p}_O, e_\omega, e_\zeta, t) := \dot{v}_f(e, t) = \begin{bmatrix} \ddot{p}_d(t) - k_p \dot{e}_p \\ \dot{\omega}_d(t) + k_\zeta \dot{e}_\zeta \end{bmatrix} \quad (27)$$

where we have implicitly used (20);  $\dot{\omega}_d(t)$  can be calculated via  $\dot{\omega}_d(t) = 2[E(\zeta_d(t))]^\top \ddot{\zeta}_d(t)$  as indicated by (2c). We also introduce the respective velocity error  $e_v$  as

$$e_{v_f} := v_O - v_f(e, t). \quad (28)$$

Denote by  $\chi_i$  the overall state  $\chi_i = [q_i^\top, \dot{q}_i^\top, x_O^\top, \dot{x}_O^\top, e_p^\top, e_\zeta^\top, e_{v_f}^\top, e_\omega^\top, e_{\vartheta_i}^\top, e_{\vartheta_{O,i}}^\top, e_{d_i}^\top, e_{d_{O,i}}^\top]^\top$  of appropriate dimension  $\mathbb{X}_i$ , and design the adaptive control law  $u_i : \mathbb{X}_i \times \mathbb{R}_{\geq 0} \rightarrow \mathbb{R}^6$  in (16), for each agent  $i \in \mathcal{N}$ , as:

$$\begin{aligned} & u_i(\chi_i, t) = [J_{O_i}(q_i)]^{-\top} \left[ Y_i(q_i, \dot{q}_i, v_f(e, t), v_f^d(\dot{p}_O, e_\omega, e_\zeta, t)) \hat{\vartheta}_i \right. \\ & \quad \left. - c_i e - K_{v_i} e_{v_f} + c_i Y_O(x_O, \dot{x}_O, v_f(e, t), v_f^d(\dot{p}_O, e_\omega, e_\zeta, t)) \hat{\vartheta}_{O_i} \right. \\ & \quad \left. + c_i \hat{d}_{O_i} \delta_O(x_O, \dot{x}_O, t) \right] + \hat{d}_i \delta_i(q_i, \dot{q}_i, t), \end{aligned} \quad (29)$$

where  $K_{v_i}$  are diagonal positive definite gain matrices,  $\forall i \in \mathcal{N}$ , and  $c_i$  are load sharing coefficients satisfying  $c_i \in (0, 1)$ ,  $\forall i \in \mathcal{N}$ , and  $\sum_{i \in \mathcal{N}} c_i = 1$ . Note that we have implicitly used the expressions  $\vartheta_i = e_{\vartheta_i} + \vartheta_i$ ,  $\hat{\vartheta}_{O_i} = e_{\vartheta_{O,i}} + \vartheta_O$ ,  $\hat{d}_i = e_{d_i} + \bar{d}_i$ ,  $\hat{d}_{O_i} = e_{d_{O,i}} + \bar{d}_O$  to express  $u_i$ ,  $i \in \mathcal{N}$ , as a function of the errors (24) and (25).

In addition, we design the following adaptation laws:

$$\dot{\theta}_i = -\gamma_i \left[ Y_i(q_i, \dot{q}_i, v_f(e, t), v_f^d(\dot{p}_o, e_\omega, e_\zeta, t)) \right]^\top e_{v_f}, \quad (30a)$$

$$\dot{\theta}_{o_i} = -c_i \gamma_{o_i} \left[ Y_o(x_o, \dot{x}_o, v_f(e, t), v_f^d(\dot{p}_o, e_\omega, e_\zeta, t)) \right]^\top e_{v_f} \quad (30b)$$

$$\dot{d}_i = -\beta_i \delta_i(q_i, \dot{q}_i, t) J_{o_i}(q_i) e_{v_f} \quad (30c)$$

$$\dot{d}_{o_i} = -c_i \beta_{o_i} \delta_o(x_o, \dot{x}_o, t) e_{v_f}, \quad (30d)$$

with arbitrary bounded initial conditions, where  $\beta_i, \beta_{o_i}, \gamma_i, \gamma_{o_i} \in \mathbb{R}_{>0}$  are positive gains,  $\forall i \in \mathcal{N}$ .

The following theorem summarizes the main results of this subsection.

**Theorem 2.** Consider  $N$  robotic agents rigidly grasping an object with coupled dynamics described by (16) and unknown dynamic parameters. Then, under Assumptions 1-4, by applying the control protocol (29) with the adaptation laws (30), the object pose converges asymptotically to the desired pose trajectory. Moreover, all closed loop signals are bounded.

*Proof:* Consider the stack state vector  $\chi := [\chi_1^\top, \dots, \chi_N^\top]^\top \in \mathbb{X} := \mathbb{X}_1 \times \dots \times \mathbb{X}_N$ , and the nonnegative function  $V: \mathbb{X} \rightarrow \mathbb{R}_{\geq 0}$ , with

$$V(\chi) := \frac{1}{2} e_p^\top e_p + 2(1 - e_\varphi) + \frac{1}{2} e_{v_f}^\top \widetilde{M}(x) e_{v_f} + \frac{1}{2} e_\vartheta^\top \Gamma^{-1} e_\vartheta + \frac{1}{2} e_{\vartheta_o}^\top \Gamma_o^{-1} e_{\vartheta_o} + \frac{1}{2} e_d^\top B^{-1} e_d + \frac{1}{2} e_{d_o}^\top B_o^{-1} e_{d_o}, \quad (31)$$

where  $B := \text{diag}\{\beta_i\}_{i \in \mathcal{N}}, B_o := \text{diag}\{\beta_{o_i}\}_{i \in \mathcal{N}}, \Gamma := \text{diag}\{\gamma_i\}_{i \in \mathcal{N}}, \Gamma_o := \text{diag}\{\gamma_{o_i}\}_{i \in \mathcal{N}}$ . Recall that the error quaternion  $e_\zeta$  as defined (19) is a unit quaternion and hence  $e_\varphi \in [-1, 1]$ .

By considering the derivatives of the elements in  $\chi$ , it can be concluded from the aforementioned dynamics that the closed loop dynamics can be written in the form  $\dot{\chi} = f_{cl}(\chi, t)$ , for a locally Lipschitz function  $f_{cl}: \mathbb{X} \times \mathbb{R}_{\geq 0} \rightarrow \mathbb{X}$ . By taking the derivative of  $V$  along the solutions of the closed loop system, we obtain

$$\begin{aligned} \dot{V}(\chi) &= e^\top (v_o - v_d(t)) + \frac{1}{2} e_{v_f}^\top \widetilde{M}(x) e_{v_f} - e_{v_f}^\top \widetilde{M}(x) \dot{v}_f \\ &+ e_{v_f}^\top \left( [G(q)]^\top u - \widetilde{C}(x) v_o - \widetilde{g}(x) - \widetilde{d}(x) \right) - e_\vartheta^\top \Gamma^{-1} \dot{\vartheta} \\ &- e_{\vartheta_o}^\top \Gamma_o^{-1} \dot{\vartheta}_o - e_d^\top B^{-1} \dot{d} - e_{d_o}^\top B_o^{-1} \dot{d}_o, \end{aligned}$$

which, by using (28) and (26), becomes

$$\begin{aligned} \dot{V}(\chi) &= -e^\top K_f e + \frac{1}{2} e_{v_f}^\top \widetilde{M}(x) e_{v_f} - e_{v_f}^\top \widetilde{C}(x) e_{v_f} \\ &+ e_{v_f}^\top \left( [G(q)]^\top u + e - \widetilde{M}(x) v_f^d(\dot{p}_o, e_\omega, e_\zeta, t) - \widetilde{g}(x) \right. \\ &\quad \left. - \widetilde{C}(x) v_f(e, t) - \widetilde{d}(x, t) \right) - e_\vartheta^\top \Gamma^{-1} \dot{\vartheta} - e_{\vartheta_o}^\top \Gamma_o^{-1} \dot{\vartheta}_o \\ &- e_d^\top B^{-1} \dot{d} - e_{d_o}^\top B_o^{-1} \dot{d}_o. \end{aligned}$$

By employing Lemma 1 as well as (23),  $\dot{V}(\chi)$  can be written as

$$\begin{aligned} \dot{V}(\chi) &= -e^\top K_f e + e_{v_f}^\top \sum_{i \in \mathcal{N}} \left[ [J_{o_i}(q_i)]^\top u_i + c_i e \right. \\ &\quad \left. - Y_o(x_o, \dot{x}_o, v_f(e, t), v_f^d(\dot{p}_o, e_\omega, e_\zeta, t)) c_i \vartheta_o \right. \\ &\quad \left. - Y_i(q_i, \dot{q}_i, v_f(e, t), v_f^d(\dot{p}_o, e_\omega, e_\zeta, t)) \theta_i - \delta_o(x_o, \dot{x}_o, t) c_i \bar{d}_o \right. \\ &\quad \left. - [J_{o_i}(q_i)]^\top \delta_i(q_i, \dot{q}_i, t) \bar{d}_i \right] - \sum_{i \in \mathcal{N}} \left( \frac{e_{\vartheta_i}}{\gamma_i} \dot{\vartheta}_i - \frac{e_{\vartheta_{o,i}}}{\gamma_{o_i}} \dot{\vartheta}_{o_i} \right. \\ &\quad \left. - \frac{e_{d_i}}{\beta_i} \dot{d}_i - \frac{e_{d_{o,i}}}{\beta_{o_i}} \dot{d}_{o_i} \right), \end{aligned}$$

and after substituting the adaptive control laws (29),

$$\begin{aligned} \dot{V}(\chi) &= -e^\top K_f e - \sum_{i \in \mathcal{N}} e_{v_f}^\top K_{v_i} e_{v_f} - \\ &e_v^\top \sum_{i \in \mathcal{N}} \left[ Y_o(x_o, \dot{x}_o, v_f(e, t), v_f^d(\dot{p}_o, e_\omega, e_\zeta, t)) c_i e_{\vartheta_{o,i}} + \right. \\ &Y_i(q_i, \dot{q}_i, v_f(e, t), v_f^d(\dot{p}_o, e_\omega, e_\zeta, t)) e_{\theta_i} + \delta_o(x_o, \dot{x}_o, t) c_i e_{d_{o,i}} \\ &\quad \left. + [J_{o_i}(q_i)]^\top \delta_i(q_i, \dot{q}_i, t) e_{d_i} \right] - \sum_{i \in \mathcal{N}} \left( \frac{e_{\vartheta_i}}{\gamma_i} \dot{\vartheta}_i - \frac{e_{\vartheta_{o,i}}}{\gamma_{o_i}} \dot{\vartheta}_{o_i} \right. \\ &\quad \left. - \frac{e_{d_i}}{\beta_i} \dot{d}_i - \frac{e_{d_{o,i}}}{\beta_{o_i}} \dot{d}_{o_i} \right), \end{aligned}$$

which, after substituting the adaptation laws (30), finally becomes

$$\begin{aligned} \dot{V}(\chi) &= -e^\top K_f e - \sum_{i \in \mathcal{N}} e_{v_f}^\top K_{v_i} e_{v_f} \\ &= -k_p \|e_p\|^2 - k_\zeta \|e_\epsilon\|^2 - \sum_{i \in \mathcal{N}} e_{v_f}^\top K_{v_i} e_{v_f}, \end{aligned}$$

which is non-positive. We conclude therefore the boundedness of  $V$  and of  $\chi$ , which implies the boundedness of the dynamic terms  $\widetilde{M}(x), \widetilde{C}(x), \widetilde{g}(x)$ . Moreover, by invoking the boundedness of  $p_d(t), v_d(t), \omega_d(t), \dot{v}_d(t), \dot{\omega}_d(t)$ , we conclude the boundedness of  $v_f(e, t), v_o, v_i, \vartheta_o, \vartheta_i, \dot{d}, \dot{d}_o$ . From (20) and (27) we also conclude the boundedness of  $\dot{v}_f(e, t)$  and therefore, the boundedness of the control and adaptation laws (29) and (30). Thus, we can conclude the boundedness of the second derivative  $\ddot{V}(\chi)$  and hence the uniform continuity of  $\dot{V}(\chi)$ . By invoking Barbalat's lemma [42], we deduce therefore that  $\lim_{t \rightarrow \infty} \dot{V}(\chi(t)) = 0$  and, consequently, that  $\lim_{t \rightarrow \infty} e_p(t) = 0_3$ ,  $\lim_{t \rightarrow \infty} e_{v_f}(t) = 0_6$ , and  $\lim_{t \rightarrow \infty} \|e_\epsilon(t)\|^2 = 0$ , which, given that  $e_\zeta$  is a unit quaternion, leads to the configuration  $(e_p, e_{v_f}, e_\varphi, e_\epsilon) = (0_3, 0_6, \pm 1, 0_3)$ . The closed loop dynamics of  $e_\varphi$ , as given in (20b), can be written, in view of (26), as  $\dot{e}_\varphi = k_\zeta \frac{1}{2} \|e_\epsilon\|^2 + \frac{1}{2} [0_3^\top, e_\epsilon^\top] e_{v_f}$ . Since the first term is always positive, we conclude that the equilibrium point  $(e_p, e_{v_f}, e_\varphi, e_\epsilon) = (0_3, 0_6, -1, 0_3)$  is unstable and, therefore, the system will converge to the configuration  $(e_p, e_{v_f}, e_\varphi, e_\epsilon) = (0_3, 0_6, 1, 0_3)$ . ■

**Remark 1** (Unwinding). Note that the two configurations where  $e_\varphi = 1$  and  $e_\varphi = -1$ , respectively, represent the same orientation. Since we restrict the system to reach the configuration where  $e_\varphi = 1$ , and the configuration where  $e_\varphi = -1$  is

unstable, we obtain the so-called unwinding phenomenon [43]. Therefore, the equilibrium  $(e_p, e_{v_f}, e_\varphi, e_\epsilon) = (0_3, 0_6, \pm 1, 0_3)$  is not stable in the classical notion, since trajectories starting close to  $e_\varphi = -1$  will move away from it and approach  $e_\varphi = 1$ , i.e., a full rotation will be performed to reach the desired orientation (of course, if the system starts at the equilibrium  $(e_p, e_{v_f}, e_\varphi, e_\epsilon) = (0_3, 0_6, -1, 0_3)$ , it will stay there, which also corresponds to the desired orientation behavior). However, the desired equilibrium point  $(e_p, e_{v_f}, e_\varphi, e_\epsilon) = (0_3, 0_6, 1, 0_3)$  is **eventually attractive**, meaning that for each  $\delta_\epsilon > 0$ , there exist finite a time instant  $T$  with  $T \geq 0$ , such that  $1 - e_\varphi(t) < \delta_\epsilon, \forall t > T \geq 0$ . A similar behavior is observed if we stabilize the point  $e_\varphi = -1$  instead of  $e_\varphi = 1$ , by setting  $e := [e_p^\top, e_\epsilon^\top]^\top$  in (26) and considering the term  $2(1 + e_\varphi)$  instead of  $2(1 - e_\varphi)$  in the Lyapunov function (31).

In order to avoid the unwinding phenomenon, instead of the error  $e = [e_p^\top, -e_\epsilon^\top]^\top$ , we can instead choose  $e = [e_p^\top, -e_\varphi e_\epsilon^\top]^\top$  (see our preliminary result [36]). Then by considering the Lyapunov function

$$V(\chi) = \frac{1}{2}e_p^\top e_p + 1 - e_\varphi^2 + \frac{1}{2}e_{v_f}^\top \widetilde{M}(x)e_{v_f} + \frac{1}{2}e_\theta^\top \Gamma^{-1}e_\theta + \frac{1}{2}e_{\vartheta_O}^\top \Gamma_O^{-1}e_{\vartheta_O} + \frac{1}{2}e_d^\top B^{-1}e_d + \frac{1}{2}e_{d_O}^\top B_O^{-1}e_{d_O},$$

and the design (26), (29), and (30), we conclude by proceeding with a similar analysis that  $(e_p, \|e_\epsilon\|e_\varphi, e_{v_f}) \rightarrow (0_3, 0, 0_6)$ , which implies that the system is asymptotically driven to either the configuration  $(e_p, e_{v_f}, e_\varphi, e_\epsilon) = (0_3, 0_6, \pm 1, 0_3)$ , which is the desired one, or a configuration  $(e_p, e_{v_f}, e_\varphi, e_\epsilon) = (0_3, 0_6, 0, \tilde{e}_\epsilon)$ , where  $\tilde{e}_\epsilon \in S^2$  is a unit vector. The latter represents a set of invariant undesired equilibrium points. The closed loop dynamics are the following:

$$\frac{\partial}{\partial t}e_\varphi = \frac{1}{2}e_\varphi\|e_\epsilon\|^2 + \frac{1}{2}[0_3^\top, e_\epsilon^\top]e_v, \quad (32a)$$

$$\frac{\partial}{\partial t}(\|e_\epsilon\|^2) = -e_\varphi^2\|e_\epsilon\|^2 - e_\varphi[0_3^\top, e_\epsilon^\top]e_v. \quad (32b)$$

We can conclude from the term  $[0_3^\top, e_\epsilon^\top]e_v$  in (32) that there exist trajectories that can bring the system close to the undesired equilibrium, rendering thus the point  $(e_p, e_{v_f}, e_\varphi, e_\epsilon) = (0_3, 0_6, \pm 1, 0_3)$  only locally asymptotically stable. It has been proven that  $e_\varphi = \pm 1$  cannot be globally stabilized with a purely continuous controller [43]. Discontinuous control laws have also been proposed (e.g., [44]), whose combination with adaptation techniques constitute part of our future research directions. Another possible direction is tracking directly on  $SO(3)$  (see e.g., [45]).

**Remark 2.** Notice also that the control protocol compensates the uncertain dynamic parameters and external disturbances through the adaptation laws (30), although the errors (24), (25) do not converge to zero, but remain bounded. Finally, the control gains  $k_p, k_\zeta, K_{v_i}$  can be tuned appropriately so that the proposed control inputs do not reach motor saturations in real scenarios.

### B. Prescribed Performance Control

In this section, we adopt the concepts and techniques of prescribed performance control, recently proposed in [38], in order to achieve predefined and transient and steady

state response for the derived error, as well as ensure that  $\theta_O(t) \in (-\frac{\pi}{2}, \frac{\pi}{2}), \forall t \in \mathbb{R}_{\geq 0}$ . As stated in Section II-C, prescribed performance characterizes the behavior where a signal evolves strictly within a predefined region that is bounded by absolutely decaying functions of time, called performance functions. This signal is represented by the object's pose error

$$e_s := \begin{bmatrix} e_{sx} \\ e_{sy} \\ e_{sz} \\ e_{s\phi} \\ e_{s\theta} \\ e_{s\psi} \end{bmatrix} := x_O - x_d(t) \quad (33)$$

First, we reformulate Assumption 4, which is now required to be less strict, stating that the functions  $d_O, d_i$  are bounded:

**Assumption 5.** (Uncertainties/Disturbance bound) There exist positive, finite unknown constants  $\bar{d}_O, \bar{d}_i$  such that

$$\begin{aligned} \|d_O(x_O, \dot{x}_O, t)\| &\leq \bar{d}_O \\ \|d_i(q_i, \dot{q}_i, t)\| &\leq \bar{d}_i \end{aligned}$$

$$\forall q_i, \dot{q}_i \in \mathbb{R}^{n_i}, x_O \in \mathbb{M}, \dot{x}_O \in \mathbb{R}^6, t \in \mathbb{R}_{\geq 0}, i \in \mathcal{N}.$$

The mathematical expressions of prescribed performance are given by the following inequalities:

$$-\rho_{s_k}(t) < e_{s_k}(t) < \rho_{s_k}(t), \forall k \in \mathcal{K}, \quad (34)$$

where  $\mathcal{K} := \{x, y, z, \phi, \theta, \psi\}$  and  $\rho_k : \mathbb{R}_{\geq 0} \rightarrow \mathbb{R}_{>0}$ , with

$$\rho_{s_k}(t) := (\rho_{s_k,0} - \rho_{s_k,\infty}) \exp(-l_{s_k} t) + \rho_{s_k,\infty}, \forall k \in \mathcal{K}, \quad (35)$$

are designer-specified, smooth, bounded and decreasing positive functions of time with  $l_{s_k}, \rho_{s_k,\infty}, k \in \mathcal{K}$ , positive parameters incorporating the desired transient and steady state performance respectively. The terms  $\rho_{s_k,\infty}$  can be set arbitrarily small, achieving thus practical convergence of the errors to zero. Next, we propose a state feedback control protocol that does not incorporate any information on the agents' or the object's dynamics or the external disturbances and guarantees (34) for all  $t \in \mathbb{R}_{\geq 0}$ . Given the errors (33):

**Step I-a.** Select the corresponding functions  $\rho_{s_k}$  as in (35) with

- (i)  $\rho_{s_\theta,0} = \rho_{s_\theta}(0) = \theta^*, \rho_{s_k,0} = \rho_{s_k}(0) > |e_{s_k}(0)|, \forall k \in \mathcal{K} \setminus \{\theta\}$ ,
- (ii)  $l_{s_k} \in \mathbb{R}_{>0}, \forall k \in \mathcal{K}$ ,
- (iii)  $\rho_{s_k,\infty} \in (0, \rho_{s_k,0}), \forall k \in \mathcal{K}$ ,

where  $\theta^*$  is a positive constant satisfying  $\theta^* + \bar{\theta} < \frac{\pi}{2}$  and  $\bar{\theta}$  is the desired trajectory bound (see statement of Problem 1)

**Step I-b.** Introduce the transformed states representing the normalized errors

$$\xi_s := \begin{bmatrix} \xi_{sx} \\ \vdots \\ \xi_{s\psi} \end{bmatrix} := [\rho_s(t)]^{-1}e_s, \quad (36)$$



where  $\rho_s(t) := \text{diag}\{[\rho_{s_k}(t)]_{k \in \mathcal{K}}\} \in \mathbb{R}^{6 \times 6}$ , as well as the transformed state functions  $\varepsilon_s : (-1, 1)^6 \rightarrow \mathbb{R}^6$ , and signals  $r_s : (-1, 1)^6 \rightarrow \mathbb{R}^{6 \times 6}$ , with

$$\varepsilon_s(\xi_s) := \begin{bmatrix} \varepsilon_{s_x}(\xi_{s_x}) \\ \vdots \\ \varepsilon_{s_\psi}(\xi_{s_\psi}) \end{bmatrix} := \begin{bmatrix} \ln\left(\frac{1+\xi_{s_x}}{1-\xi_{s_x}}\right) \\ \vdots \\ \ln\left(\frac{1+\xi_{s_\psi}}{1-\xi_{s_\psi}}\right) \end{bmatrix} \quad (37)$$

$$\begin{aligned} r_s(\xi_s) &:= \text{diag}\{[r_{s_k}]_{k \in \mathcal{K}}\} := \text{diag}\left\{\left[\frac{\partial \varepsilon_{v_k}(\xi_{s_k})}{\partial \xi_{s_k}}\right]_{k \in \mathcal{K}}\right\} \\ &= \text{diag}\left\{\left[\frac{2}{1-\xi_{s_k}^2}\right]_{k \in \mathcal{K}}\right\}, \end{aligned} \quad (38)$$

and design the reference velocity vector  $v_r : (-1, 1)^6 \times \mathbb{R}_{\geq 0} \rightarrow \mathbb{R}^6$ , with:

$$\begin{aligned} v_r(\xi_s, t) &:= \\ &- g_s J_{O, \text{inv}} \left( \eta_d(t) + \rho_{s_\eta}(t) \xi_{s_\eta} \right) [\rho_s(t)]^{-1} r_s(\xi_s) \varepsilon_s(\xi_s), \end{aligned} \quad (39)$$

where  $J_{O, \text{inv}} : \mathbb{T} \rightarrow \mathbb{R}^{6 \times 6}$  is the matrix inverse  $J_{O, \text{inv}}(\eta_O) := [J_O(\eta_O)]^{-1}$  and we have further used the relation  $\xi_s = [\rho_s(t)]^{-1}(x_O - x_d(t))$  from (33) and (36).

**Step II-a.** Define the velocity error vector

$$e_v := \begin{bmatrix} e_{v_x} \\ \vdots \\ e_{v_\psi} \end{bmatrix} := v_O - v_r(\xi_s, t), \quad (40)$$

and select the corresponding positive performance functions  $\rho_{v_k} : \mathbb{R}_{\geq 0} \rightarrow \mathbb{R}_{>0}$  with  $\rho_{v_k}(t) := (\rho_{v_k,0} - \rho_{v_k,\infty}) \exp(-l_{v_k} t) + \rho_{v_k,\infty}$ , such that  $\rho_{v_k,0} = \|e_v(0)\| + \alpha$ ,  $l_{v_k} > 0$  and  $\rho_{v_k,\infty} \in (0, \rho_{v_k,0})$ ,  $\forall k \in \mathcal{K}$ , where  $\alpha$  an arbitrary positive constant.

**Step II-b.** Define the normalized velocity error

$$\xi_v := \begin{bmatrix} \xi_{v_x} \\ \vdots \\ \xi_{v_\psi} \end{bmatrix} := [\rho_v(t)]^{-1} e_v, \quad (41)$$

where  $\rho_v(t) := \text{diag}\{[\rho_{v_k}(t)]_{k \in \mathcal{K}}\}$ , as well as the transformed states  $\varepsilon_v : (-1, 1)^6 \rightarrow \mathbb{R}^6$  and signals  $r_v : (-1, 1)^6 \rightarrow \mathbb{R}^{6 \times 6}$ , with

$$\begin{aligned} \varepsilon_v(\xi_v) &:= \begin{bmatrix} \varepsilon_{v_x}(\xi_{v_x}) \\ \vdots \\ \varepsilon_{v_\psi}(\xi_{v_\psi}) \end{bmatrix} := \begin{bmatrix} \ln\left(\frac{1+\xi_{v_x}}{1-\xi_{v_x}}\right) \\ \vdots \\ \ln\left(\frac{1+\xi_{v_\psi}}{1-\xi_{v_\psi}}\right) \end{bmatrix} \\ r_v(\xi_v) &:= \text{diag}\{[r_{v_k}]_{k \in \mathcal{K}}\} := \text{diag}\left\{\left[\frac{\partial \varepsilon_{v_k}(\xi_{v_k})}{\partial \xi_{v_k}}\right]_{k \in \mathcal{K}}\right\} \\ &= \text{diag}\left\{\left[\frac{2}{1-\xi_{v_k}^2}\right]_{k \in \mathcal{K}}\right\}, \end{aligned}$$

and design the distributed control protocol for each agent  $i \in \mathcal{N}$  as  $u_i : \mathbb{R}^{n_i} \times (-1, 1)^6 \times \mathbb{R}_{\geq 0} \rightarrow \mathbb{R}^6$ :

$$u_i(q_i, \xi_v, t) := -c_i g_v [J_{O_i}(q_i)]^\top [\rho_v(t)]^{-1} r_v(\xi_v) \varepsilon_v(\xi_v), \quad (42)$$

where  $g_v$  is a positive constant gain,  $J_{O_i}$  as defined in (12), and  $c_i$  the load sharing coefficients that were also used in (29).

The control laws (42) can be written in vector form  $u := [u_1^\top, \dots, u_N^\top]^\top$ , with:

$$u(q, \xi_v, t) = -C_g G^*(q) [\rho_v(t)]^{-1} r_v(\xi_v) \varepsilon_v(\xi_v), \quad (43)$$

where  $C_g := g_v \text{diag}\{[c_i I_{6 \times 6}]_{i \in \mathcal{N}}\} \in \mathbb{R}^{6N \times 6N}$ , and  $G^*(q) := [J_{O_1}(q_1)]^{-1}, \dots, [J_{O_N}(q_N)]^{-1}]^\top \in \mathbb{R}^{6N \times 6}$  (recall that, due to the rigidity assumption, the matrices  $J_{O_i}(q_i)$  are invertible, for all  $i \in \mathcal{N}$ ).

**Remark 3.** Notice from (29), (30), and (42) that in both control methodologies each agent  $i \in \mathcal{N}$  can calculate its own control signal, without communicating with the rest of the team, rendering thus the overall control scheme decentralized. In fact, it needs feedback only from its own state  $q_i, \dot{q}_i$ , knowledge of the object geometric characteristics, the desired object profile  $p_d(t), \eta_d(t)$ , as well as the terms  $l_k, \rho_{k,0}, \rho_{k,\infty}, \alpha, l_{v_k}$ , and  $\rho_{v_k,\infty}$ ,  $k \in \mathcal{K}$ , since the performance functions concern the object pose error and hence are common for all the agents. Moreover, both schemes guarantee robustness to uncertainties of model uncertainties and external disturbances. In particular, note that the Prescribed Performance Control protocol does not even require the structure of the terms  $\bar{M}, \bar{C}, \bar{g}, \bar{d}$ , but only the positive definiteness of  $\bar{M}$ , as will be observed in the subsequent proof of Theorem 3. It is worth noting that, in the case that one or more agent failed to participate in the task, then the remaining agents would need to appropriately update their control protocols (e.g., update the load-sharing coefficients  $c_i$ ) to compensate for the failure.

**Remark 4.** Internal force regulation can be also guaranteed by including in the control laws (29) and (42) a term of the form  $(I_{6N} - \frac{1}{N} G^*(q) [G(q)]^\top) \hat{f}_{\text{int},d}$ , where  $\hat{f}_{\text{int},d} \in \mathbb{R}^{6N}$  is a constant vector representing desired internal forces, that can be transmitted off-line to the agents. The computation, though, of  $G^*(q) [G(q)]^\top$ , by each agent, requires knowledge of all the grasping points  $p_{E_i}$ , which reduces to knowledge of the offsets  $p_{E_i/O}^O$  (since all the agents can compute  $R_O$  and  $p_O$ ), that can be also transmitted off-line to the agents.

The main results of this subsection are summarized in the following theorem.

**Theorem 3.** Consider  $N$  agents rigidly grasping an object with unknown coupled dynamics (16). Then, under Assumptions 1-3, 5, the distributed control protocol (36)-(42) guarantees that  $-\rho_{s_k}(t) < e_{s_k}(t) < \rho_{s_k}(t)$ ,  $\forall k \in \mathcal{K}, t \in \mathbb{R}_{\geq 0}$  from all the initial conditions satisfying  $|\theta(0) - \theta_d(0)| < \theta^*$  (where  $\theta^*$  was used in **Step I-a** (i)), with all closed loop signals being bounded.

*Proof:* Note first from (33), (36), (40), and (41), that the states  $x_O, v_O$  can be expressed as

$$x_O = x_d(t) + \rho_s(t) \xi_s, \quad (44a)$$

$$v_O = \rho_v(t) \xi_v + v_r(\xi_s, t), \quad (44b)$$

which was used in (39) and will be also used in the sequel.

Consider the combined state  $\sigma = [q, \xi_s, \xi_v] \in \mathbb{R}^{n+12}$ . From the differential kinematics  $v_i = J_i(q_i) \dot{q}_i$ , Assumption 3, as

well as (11) and (40), (41), we can derive

$$\begin{aligned}\dot{q} &= \tilde{J}(q)v = \tilde{J}(q)G(q)v_o \\ &= \tilde{J}(q)G(q)\left(\rho_v(t)\xi_v + v_r(\xi_s, t)\right) \\ &=: f_{cl,q}(\sigma, t),\end{aligned}\quad (45)$$

where  $\tilde{J}(q) := \text{diag}\{(J_i(q_i))^\top (J_i(q_i)(J_i(q_i))^\top)^{-1}\}_{i \in \mathcal{N}} \in \mathbb{R}^{6N \times n}$ . Next, we obtain from (36):

$$\begin{aligned}\dot{\xi}_s &= [\rho(t)]^{-1}(\dot{e} - \dot{\rho}_s(t)\xi_s), \\ &= [\rho(t)]^{-1}(\dot{x}_o - \dot{x}_d(t) - \dot{\rho}_s(t)\xi_s),\end{aligned}$$

which, after employing (8a), (33), (39), as well as (44), becomes

$$\begin{aligned}\dot{\xi}_s &= [\rho(t)]^{-1} \left[ J_o \left( \eta_d(t) + \rho_{s_\eta}(t)\xi_{s_\eta} \right) \rho_v(t)\xi_v - \dot{\rho}_s(t)\xi_s \right. \\ &\quad \left. - g_s[\rho(t)]^{-1} r_s(\xi_s)\varepsilon_s(\xi_s) - \dot{x}_d(t) \right] =: f_{cl,s}(\sigma, t).\end{aligned}\quad (46)$$

Consider now the derivative of  $J_{o,\text{inv}}(\eta_o)$  (as was defined in (39)) as  $J_{o,\text{inv}}^d : \mathbb{M} \times \mathbb{R}^6 \rightarrow \mathbb{R}^{6 \times 6}$ , with  $J_{o,\text{inv}}^d(\eta_o, \dot{x}_o) := \dot{J}_{o,\text{inv}}(\eta_o)$ , which, by employing (44), can be expressed as  $\tilde{J}_{o,\text{inv}}^d : \mathbb{R}^{n+12} \times \mathbb{R}_{\geq 0} \rightarrow \mathbb{R}^{6 \times 6}$ , with

$$\begin{aligned}\tilde{J}_{o,\text{inv}}^d(\sigma, t) &:= J_{o,\text{inv}}^d \left( \eta_d(t) + \rho_{s_\eta}(t)\xi_{s_\eta}, \right. \\ &\quad \left. J_o(\eta_d(t) + \rho_{s_\eta}(t)\xi_s)[\rho_v(t)\xi_v + v_r(\xi_s, t)] \right).\end{aligned}$$

Moreover, we define the derivative function of the signal  $r_s(\xi_s)$  as  $r_s^d : \mathbb{R}^{n+12} \times \mathbb{R}_{\geq 0} \rightarrow \mathbb{R}^{6 \times 6}$ , with  $r_s^d(\sigma, t) := \dot{r}_s(\xi_s)$ , which can be explicitly written as

$$\begin{aligned}r_s^d(\sigma, t) &= \text{diag} \left\{ \left[ \frac{2\xi_{s_k}}{(1 - \xi_{s_k})^2} \right]_{k \in \mathcal{K}} \right\} \sum_{k \in \mathcal{K}} \bar{E}_k \dot{\xi}_s \bar{e}_k \\ &= \text{diag} \left\{ \left[ \frac{2\xi_{s_k}}{(1 - \xi_{s_k})^2} \right]_{k \in \mathcal{K}} \right\} \sum_{k \in \mathcal{K}} \bar{E}_k f_{cl,s}(\sigma, t) \bar{e}_k,\end{aligned}$$

where  $\bar{E}_k \in \mathbb{R}^{6 \times 6}$  is the matrix with 1 in the position  $(k, k)$  and zeros everywhere else, and  $\bar{e}_k \in \mathbb{R}^6$  is the vector with 1 in the position  $k$  and zeros everywhere else.

Hence, we can now define the derivative of the reference velocity  $v_r$  as  $v_r^d : \mathbb{R}^{n+12} \rightarrow \mathbb{R}^6$ , with  $v_r^d(\sigma, t) := \dot{v}_r(\xi_s, t)$ , or, equivalently,

$$\begin{aligned}v_r^d(\sigma, t) &= -g_s J_{o,\text{inv}} \left( \eta_d(t) + \rho_{s_\eta}(t)\xi_s \right) \left[ [\rho_s(t)]^{-1} r_s^d(\sigma, t) \varepsilon_s(\xi_s) \right. \\ &\quad \left. + [\rho_s(t)]^{-1} [r_s(\xi_s)]^2 f_{cl,s}(\sigma, t) - [\rho_s(t)]^{-2} \dot{\rho}_s(t) r_s(\xi_s) \varepsilon_s(\xi_s) \right] \\ &\quad - g_s \tilde{J}_{o,\text{inv}}^d(\sigma, t) [\rho_s(t)]^{-1} r_s(\xi_s) \varepsilon_s(\xi_s)\end{aligned}\quad (47)$$

Moreover, from (40) and (41) one obtains:

$$\begin{aligned}\dot{\xi}_v &= [\rho_v(t)]^{-1}(\dot{e}_v - \dot{\rho}_v(t)\xi_v), \\ &= [\rho_v(t)]^{-1}(\dot{v}_o - v_r^d(\sigma, t) - \dot{\rho}_v(t)\xi_v),\end{aligned}$$

which, after employing (16), (43), and the fact that  $\sum_{i \in \mathcal{N}} c_i = 1$ , becomes

$$\begin{aligned}\dot{\xi}_v &= [\rho_v(t)]^{-1} \left( -\dot{\rho}_v(t)\xi_v - \widetilde{M}(x(\sigma, t)) \left[ \widetilde{C}(x(\sigma, t)) [\rho_v(t)\xi_v + \right. \right. \\ &\quad \left. \left. v_r(\xi_s, t)] + \widetilde{g}(x(\sigma, t)) + \widetilde{d}(x(\sigma, t), t) - \right. \right. \\ &\quad \left. \left. g_v[\rho_v(t)]^{-1} r_v(\xi_v) \varepsilon_v(\xi_v) \right] - v_r^d(\sigma, t) \right) =: f_{cl,v}(\sigma, t)\end{aligned}\quad (48)$$

and where, with a slight abuse of notation and by using (44) and (45), we have written  $x$  (that was first defined in (16)) as a function of  $\sigma$  and  $t$ , i.e.,

$$x(\sigma, t) = \begin{bmatrix} q \\ \dot{q} \\ x_o \\ \dot{x}_o \end{bmatrix} = \begin{bmatrix} q \\ f_{cl,q}(\sigma, t) \\ x_d(t) + \rho_s(t)\xi_s \\ J_o \left( \eta_d(t) + \rho_{s_\eta}(t)\xi_{s_\eta} \right) [\rho_v(t)\xi_v + v_r(\xi_s, t)] \end{bmatrix}.$$

Hence, we can write (45)-(48) in compact form

$$\dot{\sigma} = f_{cl}(\sigma, t) := \begin{bmatrix} f_{cl,q}(\sigma, t) \\ f_{cl,s}(\sigma, t) \\ f_{cl,v}(\sigma, t) \end{bmatrix}.$$

Consider now the open and nonempty set  $\Omega := \mathbb{R}^n \times (-1, 1)^{12}$ . The choice of the parameters  $\rho_{s_k,0}$  and  $\rho_{v_k,0}$ ,  $k \in \mathcal{K}$  in **Step I-a** and **Step II-a**, respectively, along with the fact that the initial conditions satisfy  $|\theta_o(0) - \theta_d(0)| < \theta^*$  imply that  $|e_{s_k}(0)| < \rho_{s_k}(0)$ ,  $|e_{v_k}(0)| < \rho_{v_k}(0)$ ,  $\forall k \in \mathcal{K}$  and hence  $[[\xi_s(0)]^\top, [\xi_v(0)]^\top]^\top \in (-1, 1)^{12}$ . Moreover, it can be verified that  $f_{cl} : \Omega \times \mathbb{R}_{\geq 0} \rightarrow \mathbb{R}^{n+12}$  is locally Lipschitz in  $\sigma$  over the set  $\Omega$  and is continuous in  $t$ , which makes it also locally integrable in  $t$  for each fixed  $\sigma \in \Omega$ . Therefore, the hypotheses of Theorem 1 stated in Subsection II-D hold and the existence of a maximal solution  $\sigma : [0, \tau_{\max}) \rightarrow \Omega$ , for  $\tau_{\max} > 0$ , is ensured. We thus conclude that

$$\xi_{s_k}(t) = \frac{e_{s_k}(t)}{\rho_{s_k}(t)} \in (-1, 1), \quad (49a)$$

$$\xi_{v_k}(t) = \frac{e_{v_k}(t)}{\rho_{v_k}(t)} \in (-1, 1), \quad (49b)$$

$\forall k \in \mathcal{K}, t \in [0, \tau_{\max})$ , which also implies that  $\|\xi_s(t)\| \leq \sqrt{6}$ , and  $\|\xi_v(t)\| \leq \sqrt{6}, \forall t \in [0, \tau_{\max})$ . Next, we need to show the boundedness of all closed loop signals as well as that  $\tau_{\max} = \infty$ . Note first from (49), that  $|\theta_o(t) - \theta_d(t)| < \rho_\theta(t) \leq \rho_\theta(0) = \theta^*$ , which, since  $\theta_d(t) \in [-\bar{\theta}, \bar{\theta}], \forall t \in \mathbb{R}_{\geq 0}$ , implies that  $|\theta_o(t)| \leq \bar{\theta} := \bar{\theta} + \theta^* < \frac{\pi}{2}, \forall t \in [0, \tau_{\max})$ . Therefore, by employing (9), one obtains

$$\|J_o(\eta_o(t))\| \leq \bar{J}_o := \sqrt{\frac{|\sin(\bar{\theta})| + 1}{1 - \sin^2(\bar{\theta})}} < \infty, \quad \forall t \in [0, \tau_{\max}). \quad (50)$$

Consider now the positive definite and radially unbounded function  $V_s : \mathbb{R}^6 \rightarrow \mathbb{R}_{\geq 0}$ , with  $V_s(\varepsilon_s(\xi_s)) = \frac{1}{2} \|\varepsilon_s(\xi_s)\|^2$ , and its derivative along the solutions of the closed loop system, which, in view of (46), yields

$$\begin{aligned}\dot{V}_s(\varepsilon_s(\xi_s)) &= -g_s \|[\rho_s(t)]^{-1} r_s(\xi_s) \varepsilon_s(\xi_s)\|^2 + \\ &\quad [\varepsilon_s(\xi_s)]^\top r_s(\xi_s) [\rho_s(t)]^{-1} \left( J_o(\eta_d(t) + \rho_{s_\eta}(t)\xi_{s_\eta}) \rho_v(t)\xi_v \right. \\ &\quad \left. - \dot{x}_d(t) - \dot{\rho}_s(t)\xi_s \right) \\ &\leq g_s \|[\rho(t)]^{-1} r_s(\xi_s) \varepsilon_s(\xi_s)\|^2 + \\ &\quad \|[\rho_s(t)]^{-1} r_s(\xi_s) \varepsilon_s(\xi_s)\| \left( \|J_o(\eta_d(t) + \rho_{s_\eta}(t)\xi_{s_\eta}) \rho_v(t)\xi_v\| \right. \\ &\quad \left. + \|\dot{x}_d(t)\| + \|\dot{\rho}_s(t)\xi_s\| \right).\end{aligned}$$

In view of (50), (49), and the structure of  $\rho_{s_k}, \rho_{v_k}, k \in \mathcal{K}$ , as well as the fact that  $v_o(0) = 0$  and the boundedness of  $\dot{x}_d(t)$ , the last inequality becomes

$$\dot{V}_s(\varepsilon_s(\xi_s)) \leq -g_s \|[\rho_s(t)]^{-1} r_s(\xi_s(t)) \varepsilon_s(\xi_s(t))\|^2 + \|[\rho_s(t)]^{-1} r_s(\xi_s(t)) \varepsilon_s(\xi_s(t))\| \bar{B}_s,$$

$\forall t \in [0, \tau_{\max})$ , where

$$\bar{B}_s := \sqrt{6} \bar{J}_o (\|v_r^0\| + \alpha) + \bar{x}_d + \sqrt{6} \max_{k \in \mathcal{K}} \{l_k(\rho_{s_k,0} - \rho_{s_k,\infty})\},$$

is a positive constant independent of  $\tau_{\max}$ ,  $\bar{x}_d$  is the bound of  $\dot{x}_d(t)$ , and  $v_r^0 := v_r(\xi_s(0), 0)$ . Therefore,  $\dot{V}_s(\varepsilon_s(\xi_s))$  is negative when  $\|[\rho_s(t)]^{-1} r_s(\xi_s(t)) \varepsilon_s(\xi_s(t))\| > \frac{\bar{B}_s}{g_s}$ , which, by employing (38), the decreasing property of  $\rho_{s_k}(t), k \in \mathcal{K}$  as well as (49a), is satisfied when  $\|\varepsilon_s(\xi_s(t))\| > \frac{\max_{k \in \mathcal{K}} \{\rho_{s_k,0}\} \bar{B}_s}{2g_s}$ . Hence, we conclude that

$$\|\varepsilon_s(\xi_s(t))\| \leq \bar{\varepsilon}_s := \max \left\{ \|\varepsilon_s(\xi_s(0))\|, \frac{\max_{k \in \mathcal{K}} \{\rho_{s_k,0}\} \bar{B}_s}{2g_s} \right\}, \quad (51)$$

$\forall t \in [0, \tau_{\max})$ . Furthermore, since  $|\varepsilon_{s_k}(\xi_{s_k})| \leq \|\varepsilon_s(\xi_s)\|, \forall k \in \mathcal{K}$ , taking the inverse logarithm function from (37), we obtain

$$-1 < \frac{\exp(-\bar{\varepsilon}_s) - 1}{\exp(-\bar{\varepsilon}_s) + 1} =: -\bar{\xi}_s \leq \xi_{s_k}(t) \leq \bar{\xi}_s := \frac{\exp(\bar{\varepsilon}_s) - 1}{\exp(\bar{\varepsilon}_s) + 1} < 1, \quad (52)$$

$\forall t \in [0, \tau_{\max})$ . Hence, recalling (38), one obtains

$$\|r_s(\xi_s(t))\| \leq \bar{r}_s := \frac{2}{1 - \bar{\xi}_s^2} = \frac{(\exp(\bar{\varepsilon}_s) + 1)^2}{2 \exp(\bar{\varepsilon}_s)},$$

$\forall t \in [0, \tau_{\max})$ . Therefore, we obtain from (39) the boundedness of  $v_r$  with

$$\|v_r(\xi_s(t), t)\| \leq \bar{v}_r := g_s \bar{J}_o \frac{\bar{\varepsilon}_s (\exp(\bar{\varepsilon}_s) + 1)^2}{2 \min_{k \in \mathcal{K}} \{\rho_{s_k,\infty}\} \exp(\bar{\varepsilon}_s)}, \quad (53)$$

$\forall t \in [0, \tau_{\max})$ . Since  $v_o = v_r(\xi_s, t) + \rho_v(t) \xi_v$ , we also conclude that

$$\|v_o(t)\| \leq \bar{v}_o := g_s \bar{J}_o \frac{\bar{\varepsilon}_s (\exp(\bar{\varepsilon}_s) + 1)^2}{2 \min_{k \in \mathcal{K}} \{\rho_{k,\infty}\} \exp(\bar{\varepsilon}_s)} + \sqrt{6} \max_{k \in \mathcal{K}} \{\rho_{v_k,0}\}, \quad (54)$$

$\forall t \in [0, \tau_{\max})$ , which, through (11) and (14), leads to

$$\|v_i(t)\| \leq \bar{v}_i := (\|p_{o/E_i}^{E_i}\| + 1) \bar{v}_o, \forall i \in \mathcal{N}, t \in [0, \tau_{\max}). \quad (55)$$

In a similar vein, we can also derive a bound for the derivative of the reference velocity (47),  $\|v_r^d(\sigma(t), t)\| \leq \bar{v}_r^d, \forall t \in [0, \tau_{\max})$ , which is not written explicitly for presentation clarity. From (52) and (33) we also conclude that  $\|x_o(t)\| \leq \bar{x}_o := \bar{x}_d + \sqrt{6} \bar{\xi}_s \max_{k \in \mathcal{K}} \{\rho_{s_k,0}\}, t \in [0, \tau_{\max})$ .

Applying the aforementioned line of proof, we consider the positive definite and radially unbounded function  $V_v : \mathbb{R}^6 \rightarrow \mathbb{R}_{\geq 0}$ , with  $V_v(\varepsilon_v(\xi_v)) = \frac{1}{2} \|\varepsilon_v(\xi_v)\|^2$ , and its derivative along

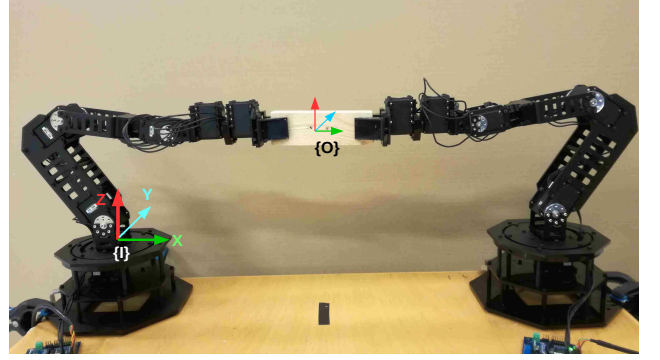


Fig. 2: Two WidowX Robot Arms rigidly grasping an object.

the solutions of the closed loop system, which, in view of (48), yields

$$\begin{aligned} \dot{V}_v(\varepsilon_v(\xi_v)) &= -g_v [\varepsilon_v(\xi_v)]^\top r_v(\xi_v) [\rho_v(t)]^{-1} \widetilde{M}(x(\sigma, t)) \cdot \\ &[\rho_v(t)]^{-1} r_v(\xi_v) \varepsilon_v(\xi_v) + [\varepsilon_v(\xi_v)]^\top r_v(\xi_v) [\rho_v(t)]^{-1} \left( -\dot{\rho}_v(t) \xi_v \right. \\ &\quad \left. - \widetilde{M}(x(\sigma, t)) [\widetilde{C}(x(\sigma, t)) [\rho_v(t) \xi_v + v_r(\xi_s, t)] + \widetilde{g}(x(\sigma, t)) \right. \\ &\quad \left. + \widetilde{d}(x(\sigma, t), t)] - v_r^d(\sigma, t) \right), \end{aligned} \quad (56)$$

From Assumption 5, expressions (14), and (17d), we obtain  $\|\widetilde{d}(x(\sigma(t), t))\| \leq \bar{d} := \bar{d}_o + \sum_{i \in \mathcal{N}} \{\|p_{o/E_i}^{E_i}\| + 1\} \bar{d}_i$ . Moreover, by using (10) and the fact that the rotation matrix  $R_{E_i}(q_i)$  is an orthogonal matrix, we obtain  $\|x_{E_i}(t)\| := \|p_{E_i}^\top(t), \eta_{E_i}^\top(q_i(t))\| \leq \|x_o(t)\| + \|(p_{E_i/o}^{E_i}, \eta_{E_i/o}^\top)^\top\|$  and hence, in view of the inverse kinematics of the agents [37], we conclude the boundedness of  $q(t)$  as

$$\|q(t)\| \leq \bar{q}, \forall t \in [0, \tau_{\max}), \quad (57)$$

where  $\bar{q}$  is a positive constant. From Assumption 3 and the forward differential agent kinematics, we can also conclude that there exists a positive constant  $\bar{J}$  such that  $\|\dot{q}(t)\| \leq \bar{J} \|v\| \leq \bar{J} \sum_{i \in \mathcal{N}} \bar{v}_i, \forall t \in [0, \tau_{\max})$ , where  $\bar{v}_i$  was defined in (55). Therefore, we conclude that

$$\|x(\sigma(t), t)\| \leq \bar{x} := \bar{q} + \bar{J} \sum_{i \in \mathcal{N}} \bar{v}_i + \bar{x}_o + \bar{J}_o \bar{v}_o, \quad (58)$$

$\forall t \in [0, \tau_{\max})$ . Hence, since the terms  $\widetilde{C}(x), \widetilde{g}(x)$  are continuous  $\forall x \in \mathbb{R}^{2n+6} \times \mathbb{M}$ , we conclude from (58) that there exist positive constants  $\bar{c}, \bar{g}$ , independent of  $\tau_{\max}$  (since  $\bar{x}$  is also independent of  $\tau_{\max}$ ), such that  $\|\widetilde{C}(x(\sigma(t), t))\| \leq \bar{c}, \|\widetilde{g}(x(\sigma(t), t))\| \leq \bar{g}, \forall t \in [0, \tau_{\max})$ .

Thus, by combining the aforementioned results along with the boundedness of  $v_r$ , (49), (53), (58) as well as (18), we obtain from (56)

$$\begin{aligned} \dot{V}_v(\varepsilon_v(\xi_v)) &\leq -g_v \underline{m} \|[\rho_v(t)]^{-1} r_v(\xi_v(t)) \varepsilon_v(\xi_v(t))\|^2 + \\ &\|[\rho_v(t)]^{-1} r_v(\xi_v(t)) \varepsilon_v(\xi_v(t))\| \bar{B}_v, \end{aligned}$$

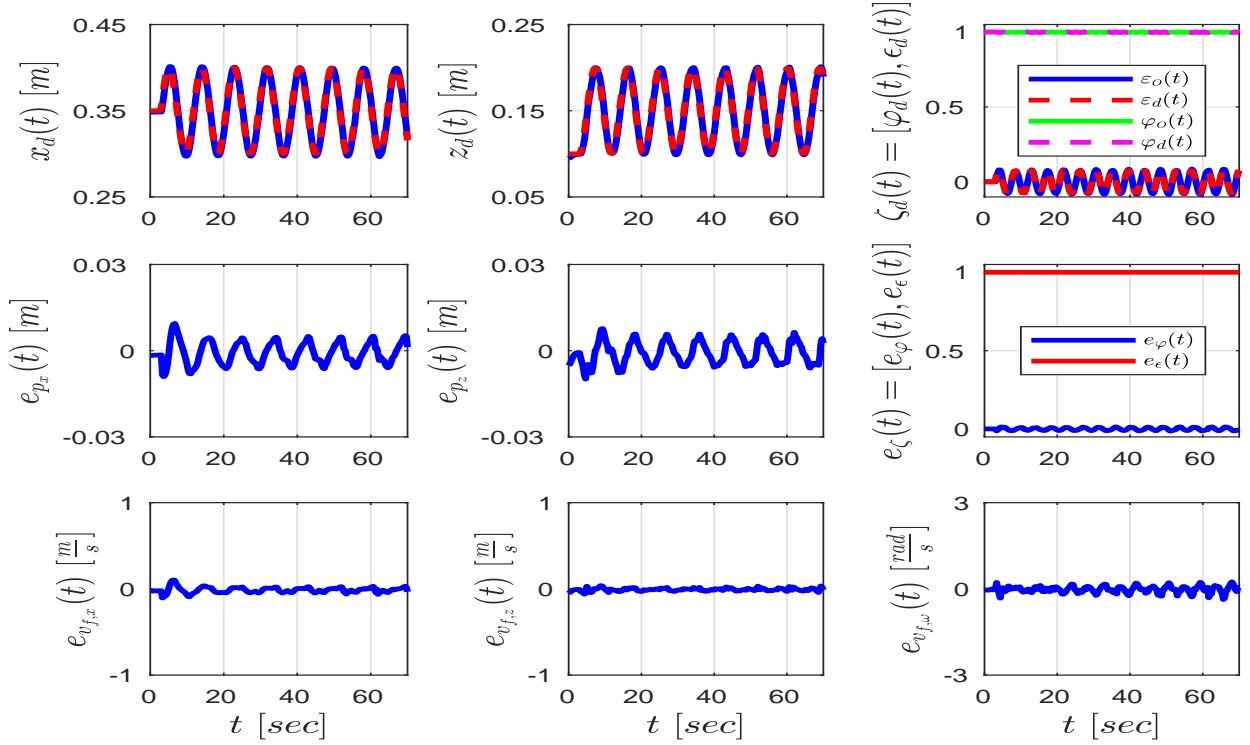


Fig. 3: Simulations results for the controller of subsection IV-A, for  $t \in [0, 70]$  [sec]. Top: The desired (with blue) and actual (with red) object trajectory in  $x$ - and  $z$ -axis as well as the quaternion desired and actual object trajectory. Middle: The position and quaternion errors  $e_p(t)$ ,  $e_{\zeta}(t)$ , respectively. Bottom: The velocity errors  $e_{v_f}(t)$ .

$\forall t \in [0, \tau_{\max})$ , where

$$\bar{B}_v := \sqrt{6} \max_{k \in \mathcal{K}} \{l_{v_k}(\rho_{v_k,0} - \rho_{v_k,\infty})\} + \bar{v}_r^d + \bar{m}(\bar{g} + \bar{d} + \bar{c}(\bar{v}_r + \sqrt{6}(\|v_r^0\| + \alpha))). \quad (59)$$

By proceeding similarly as with  $\dot{V}(\varepsilon_s(\xi_s))$ , we conclude that

$$\|\varepsilon_v(\xi_v(t))\| \leq \bar{\varepsilon}_v := \max \left\{ \|\varepsilon_v(\xi_v(0))\|, \frac{\max_{k \in \mathcal{K}} \{\rho_{v_k,0}\} \bar{B}_v}{2g_v \bar{m}} \right\}, \quad (60)$$

$\forall t \in [0, \tau_{\max})$ , from which we obtain

$$-1 < \frac{\exp(-\bar{\varepsilon}_v) - 1}{\exp(-\bar{\varepsilon}_v) + 1} =: -\bar{\xi}_v \leq \xi_{v_k}(t) \leq \bar{\xi}_v := \frac{\exp(\bar{\varepsilon}_v) - 1}{\exp(\bar{\varepsilon}_v) + 1} < 1, \quad (61)$$

as well as

$$\|r_v(\xi_v(t))\| \leq \bar{r}_v := \frac{2}{1 - \bar{\xi}_v^2} = \frac{(\exp(\bar{\varepsilon}_v) + 1)^2}{2 \exp(\bar{\varepsilon}_v)},$$

$\forall t \in [0, \tau_{\max})$ . Hence, we can also conclude the boundedness of the control inputs (42)

$$\|u_i(q_i(t), \xi_v(t), t)\| \leq \bar{u}_i := c_i g_v (\|p_{O/E_i}^{E_i}\| + 1) \max_{k \in \mathcal{K}} \left\{ \frac{1}{\rho_{v_k,\infty}} \right\} \bar{r}_v \bar{\varepsilon}_v, \quad \forall t \in [0, \tau_{\max}). \quad (62)$$

What remains to be shown is that  $\tau_{\max} = \infty$ . To this end, note from (57), (52), (61), that the solution  $\sigma(t)$  remains in a compact subset of  $\Omega = \mathbb{R}^n \times (-1, 1)^{12}$ , i.e.,

$$\sigma(t) \in \Omega' := [-\bar{q}, \bar{q}] \times [-\bar{\xi}_s, \bar{\xi}_s]^6 \times [-\bar{\xi}_v, \bar{\xi}_v]^6,$$

$\forall t \in [0, \tau_{\max})$ . Hence, assuming  $\tau_{\max} < \infty$  and since  $\Omega' \subset \Omega$ , Proposition 1 in Subsection II-D dictates the existence of a time instant  $t' \in [0, \tau_{\max})$  such that  $\sigma(t') \notin \Omega'$ , which is a contradiction. Therefore,  $\tau_{\max} = \infty$ . Thus, all closed loop signals remain bounded and moreover  $\sigma(t) \in \Omega' \subset \Omega, \forall t \in \mathbb{R}_{\geq 0}$ . Finally, by multiplying (52) by  $\rho_k(t), k \in \mathcal{K}$ , we obtain

$$-\rho_{s_k}(t) < -\bar{\xi}_s \rho_{s_k}(t) \leq e_{s_k}(t) \leq \bar{\xi}_s \rho_{s_k}(t) < \rho_{s_k}(t), \quad (63)$$

$\forall t \in \mathbb{R}_{\geq 0}$ , which leads to the conclusion of the proof. ■

**Remark 5.** From the aforementioned proof it can be deduced that the Prescribed Performance Control scheme achieves its goal without resorting to the need of rendering the ultimate bounds  $\bar{\varepsilon}_s, \bar{\varepsilon}_v$  of the modulated pose and velocity errors  $\varepsilon_s(\xi_s(t)), \varepsilon_v(\xi_v(t))$  arbitrarily small by adopting extreme values of the control gains  $g_s$  and  $g_v$  (see (51) and (60)). More specifically, notice that (52) and (61) hold no matter how large the finite bounds  $\bar{\varepsilon}_s, \bar{\varepsilon}_v$  are. In the same spirit, large uncertainties involved in the coupled model (16) can be compensated, as they affect only the size of  $\varepsilon_v$  through  $\bar{B}_v$  (see (59)), but leave unaltered the achieved stability properties. Hence, the actual performance given in (63), which is solely determined by the designed-specified performance functions  $\rho_{s_k}(t), \rho_{v_k}(t), k \in \mathcal{K}$ , becomes isolated against model uncertainties, thus extending greatly the robustness of the proposed control scheme.

**Remark 6 (Control Input Bounds).** The aforementioned analysis of the Prescribed Performance Control methodology reveals the derivation of implicit bounds for the velocity  $v_i$



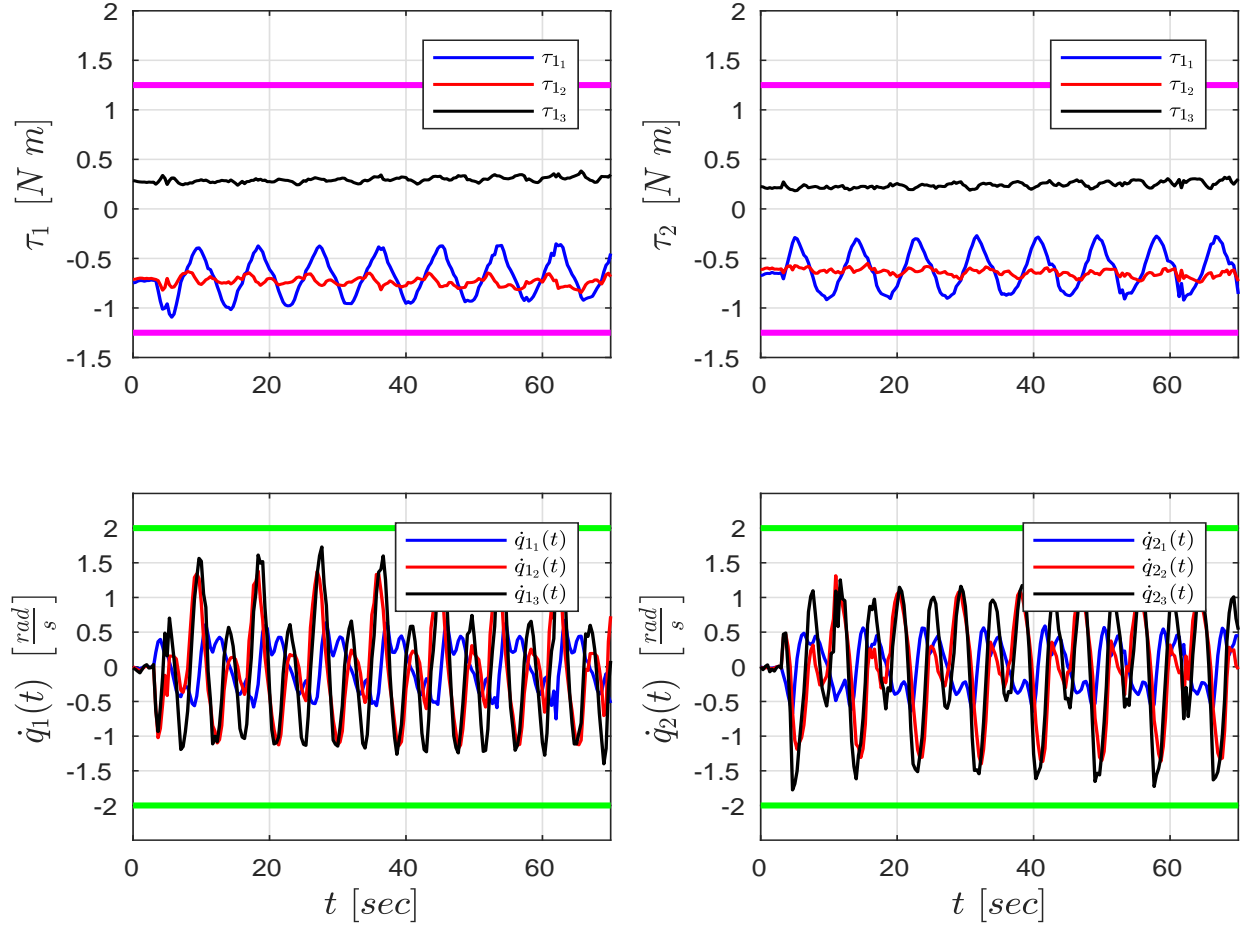


Fig. 4: The agent joint torques and velocities of the simulation of the controller in subsection IV-A, for  $t \in [0, 70]$  [sec], with their respective limits (purple and green lines, respectively). Top: The joint torques of agent 1 (left) and agent 2 (right). Bottom: The joint velocities of agent 1 (left) and agent 2 (right).

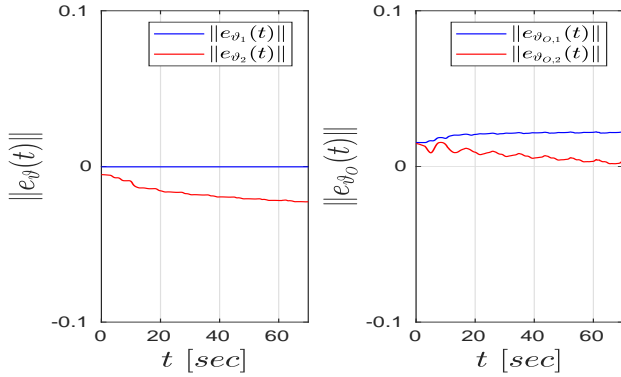


Fig. 5: The norms of the adaptation signals  $e_{\vartheta_i}(t)$  (left) and  $e_{\vartheta_{o,i}}(t)$ ,  $\forall i \in \{1, 2\}, t \in [0, 70]$  [sec] of the simulation of the controller in subsection IV-A.

and control input  $u_i$  of each agent. More specifically, notice that (55) and (54) provide a bound for the agents' velocity,  $\|v_i(t)\| \leq \bar{v}_i$ . Therefore, given a bound for the agents' velocity  $\bar{v}_{i,b}$  (derived from bounds on the joint velocities  $\dot{q}_i$ ),  $i \in \mathcal{N}$ , the desired trajectory velocity bound  $\bar{x}_d$ , as well as the initial velocity error  $v_r^0$  (which is proportional to  $\varepsilon_s(\xi_s(0))$ ),

we can tune appropriately the control gain  $g_s$  as well as the parameters  $\rho_{s_k,0}, \rho_{v_k,0}, \rho_{s_k,\infty}, \rho_{v_k,\infty}, l_{s_k}, l_{v_k}$ , and  $\alpha$ , to achieve  $\bar{v}_i \leq \bar{v}_{i,b}, \forall i \in \mathcal{N}$ . In the same spirit, (62) provides a bound  $\bar{u}_i$  for the control inputs of the agents. Hence, given bounds for the agents' inputs  $\bar{u}_{i,b}$  (derived from bounds on the joint torques  $\tau_i$ ),  $i \in \mathcal{N}$ , if the upper bound term  $\bar{B}_v$  is known, we can further tune the control gain  $g_v$  as well as the performance function parameters to achieve  $\bar{u} \leq \bar{u}_{i,b}$ . Explicit closed-loop expressions for the choice of these gains and parameters are beyond the scope of this paper and consist part of future work. It is also worth noting that the selection of the control gains  $g_s, g_v$  affects the evolution of the errors  $e, e_v$  inside the corresponding performance envelope.

## V. SIMULATION AND EXPERIMENTAL RESULTS

In this section, we provide simulation and experimental results for the two develop control schemes. Firstly, in subsection V-A we present results from computer simulations using the realistic environment of V-REP [46] as well as experimental results using the adaptive control protocol developed in Section IV-A. Then, in subsection V-B, we provide simulation and experimental results using the Prescribed Performance Control algorithm developed in Section IV-B.

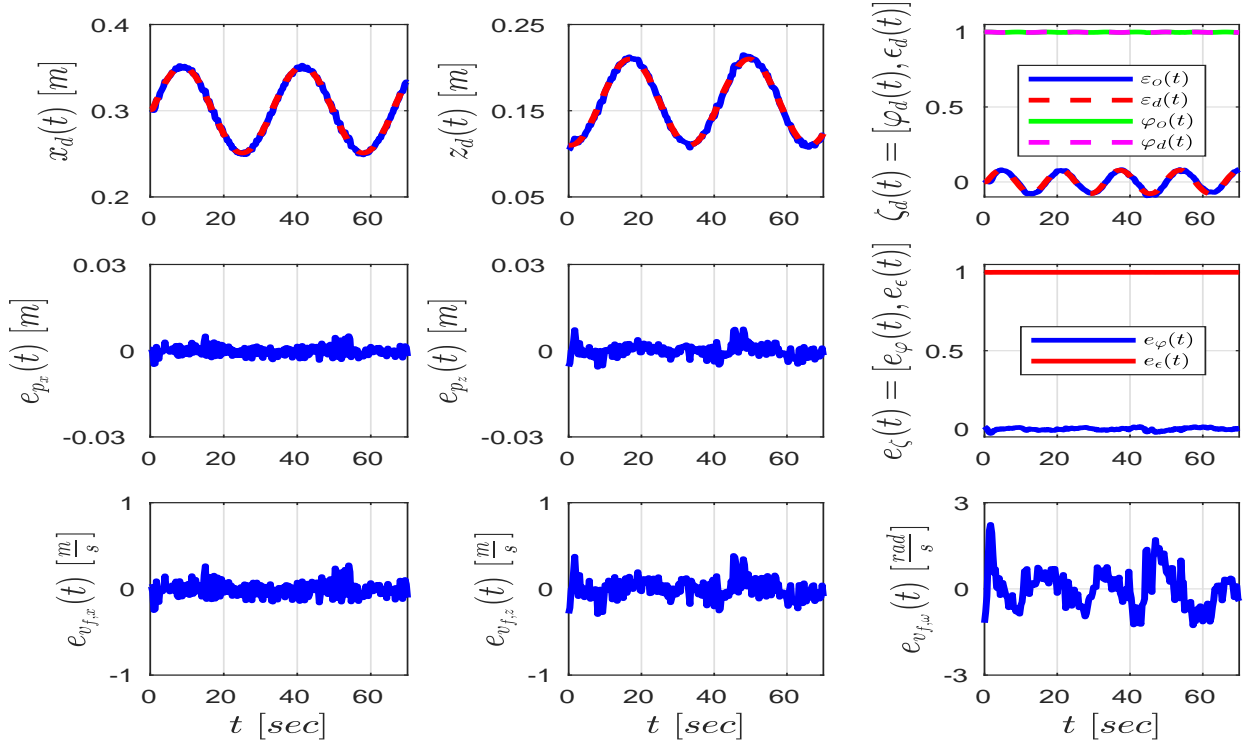


Fig. 6: Experimental results for the controller of subsection IV-A, for  $t \in [0, 70]$  [sec]. Top: The desired (with blue) and actual (with red) object trajectory in  $x$ - and  $z$ -axis as well as the quaternion desired and actual object trajectory. Middle: The position and quaternion errors  $e_p(t)$ ,  $e_{\zeta}(t)$ , respectively. Bottom: The velocity errors  $e_{v_f}(t)$ .

The tested scenario consists of two WidowX Robot Arms [47] rigidly grasping a wooden cuboid object (see Fig. 2) that has to track a planar time trajectory  $p_d(t) = [x_d(t), 0, z_d(t)]^\top$ ,  $\eta_d(t) = [0, \theta_d(t), 0]^\top$ . For that purpose, we employ the three rotational -with respect to the  $y$  axis - joints of the arms. The lower joint consists of a MX-64 Dynamixel Actuator, whereas each of the two upper joints consists of a MX-28 Dynamixel Actuator from the MX Series [48]. Both actuators provide feedback of the joint angle and rate  $q_i, \dot{q}_i$ ,  $\forall i \in \{1, 2\}$ . The micro-controller used for the actuators of each arm is the ArbotiX-M Robocontroller [49], which is serially connected to a i-7 desktop computer with 4 cores and 16GB RAM. All the computations for the real-time experiments are performed at a frequency of 120 [Hz] and for the V-REP simulations at 60 [Hz]. Finally, we consider that the MX-64 motor can exert a maximum torque of 3 [Nm], and the MX-28 motors can exert a maximum torque of 1.25 [Nm], values that are slightly more conservative than the actual limits. In the same vein, we also assume a velocity bound of 0.5 [rad/s] for the experiments and 2 [rad/s] for the V-REP simulations. In all cases, we set the load sharing coefficients at  $c_1 = 0.75$  and  $c_2 = 0.25$ , in order to demonstrate a potential difference in the power capabilities of the agents. A video illustrating the simulation and experimental results accompanies the specific paper.

#### A. Adaptive Control with Quaternion Feedback

In this subsection, we present simulation and experimental results for the control protocol developed in Section IV-A.

1) *Simulation Results:* The desired trajectory for the V-REP simulations is set to  $x_d(t) = 0.35 + 0.05 \sin\left(\frac{2\pi t}{15}\right)$  [m],  $z_d(t) = 0.15 - 0.05 \cos\left(\frac{2\pi t}{15}\right)$  [m], which defines a circle in the  $x$ - $z$  plane of center (0.35, 0.15) [m] and radius 0.05 [m], and  $\theta_d(t) = \frac{\pi}{20} \sin\left(\frac{5\pi t}{15}\right)$  [rad], which is translated to the desired 2D quaternion trajectory  $\zeta_d(t) = \left[\cos\left(\frac{\theta_d(t)}{2}\right), 0, 0, \sin\left(\frac{\theta_d(t)}{2}\right)\right]^\top$ . The simulation results are depicted in Figs. 3-5 for  $t \in [0, 70]$  [sec]; Fig. 3 pictures the desired and actual trajectory of the object's center of mass (top), the pose errors  $e_p(t)$ ,  $e_{\zeta}(t)$  (middle), as well as the velocity error  $e_{v_f}(t)$  (bottom). We can verify from the figure that the desired trajectory is tracked almost perfectly, with negligible oscillations. The control inputs as well as the agent velocities with their respective limits are illustrated in Fig. 4. By appropriately tuning the control gains, which were set as  $k_p = 15$ ,  $k_{\zeta} = 30$ ,  $K_{v_1} = K_{v_2} = \text{diag}\{5, 2, 0.1\}$ , we achieved confinement of the signals in the domain formed by the limits. Note also the difference due to the different load sharing coefficients. Finally, Fig. 3 depicts the norms of the adaptation signals  $e_{\vartheta_i}(t)$  and  $e_{\vartheta_{O_i}}(t)$ ,  $\forall i \in \{1, 2\}$ , which, as proven in the theoretical analysis, remain bounded. The functions  $\delta_o(x_o, \dot{x}_o, t)$ ,  $\delta_i(q_i, \dot{q}_i, t)$  were taken as  $0_6$  and  $0_{n_i}$ , respectively, and hence, the adaptation controller (30c), (30d) were not employed. Loosely speaking, the disturbances  $d_o(x_o, \dot{x}_o, t)$ ,  $d_i(q_i, \dot{q}_i, t)$  were not taken into account in our model, without, however, degrading the performance of the proposed scheme.

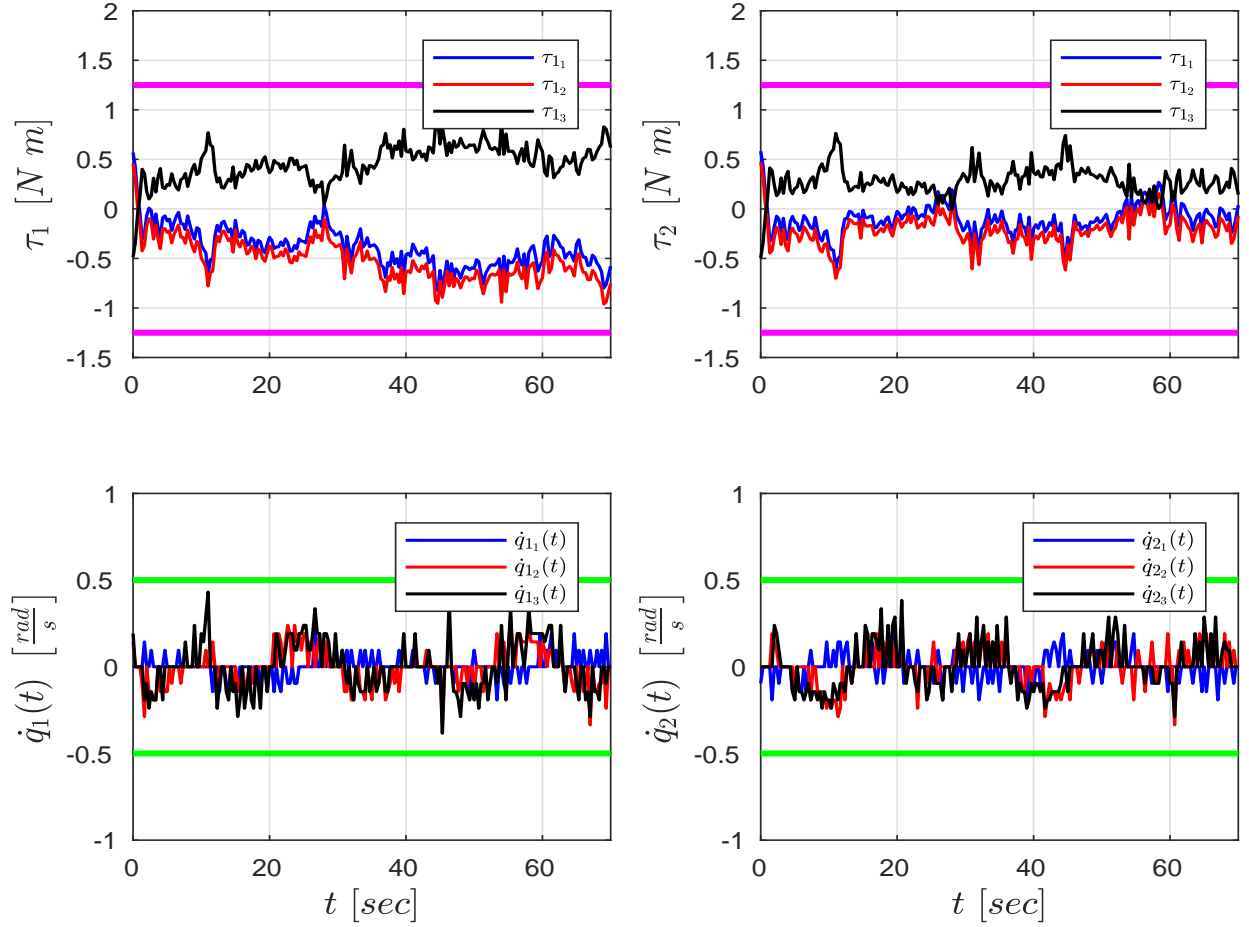


Fig. 7: The agent joint torques and velocities of the experiment of the controller in subsection IV-A, for  $t \in [0, 70]$  [sec], with their respective limits (purple and green lines, respectively). Top: The joint torques of agent 1 (left) and agent 2 (right). Bottom: The joint velocities of agent 1 (left) and agent 2 (right).

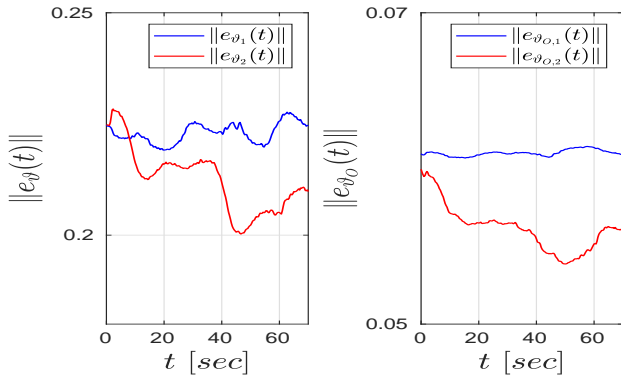


Fig. 8: The norms of the adaptation signals  $e_{\vartheta_i}(t)$  (left) and  $e_{\vartheta_{O,i}}(t)$ ,  $\forall i \in \{1, 2\}$ ,  $t \in [0, 70]$  [sec] of the experiment of the controller in subsection IV-A.

2) *Experimental Results:* The desired trajectory for the experimental results of the controller developed in Section IV-A was set to  $x_d(t) = 0.3 + 0.05 \sin\left(\frac{2\pi t}{35}\right)$  [m],  $z_d(t) = 0.15 - 0.05 \cos\left(\frac{2\pi t}{35}\right)$  [m], which defines a similar circle with the simulations section, and  $\theta_d(t) = \frac{\pi}{20} \sin\left(\frac{5\pi t}{35}\right)$  [rad], which is translated to the corresponding desired 2D quarter-

nion trajectory  $\zeta_d(t) = \left[ \cos\left(\frac{\theta_d(t)}{2}\right), 0, 0, \sin\left(\frac{\theta_d(t)}{2}\right) \right]^\top$ . The control gains here were chosen as  $k_p = 50$ ,  $k_\zeta = 80$ ,  $K_{v_1} = K_{v_2} = \text{diag}\{3.5, 0.5, 0.5\}$ . The disturbances  $d_O(x_O, \dot{x}_O, t)$ ,  $d_i(q_i, \dot{q}_i, t)$  were also not taken into account in this case, by setting the functions  $\delta_O(x_O, \dot{x}_O, t)$ ,  $\delta_i(q_i, \dot{q}_i, t)$  to 0<sub>6</sub> and 0 <sub>$n_i$</sub> , respectively. The simulation results are depicted in Figs. 6-8 for  $t \in [0, 70]$  [sec]; Fig. 6 pictures the desired and actual trajectory of the object's center of mass (top), the pose errors  $e_p(t)$ ,  $e_\zeta(t)$  (middle), as well as the velocity error  $e_{v_f}(t)$  (bottom). We can verify from the figure that the desired trajectory is tracked also for the experimental case, with oscillations in the velocity errors, which can be attributed to model uncertainties, sensor noise, or the unmodeled external disturbances, that have a larger effect in this (experimental) scenario. The control inputs as well as the agent velocities with their respective limits are illustrated in Fig. 7, which are confined in their respective limits. Finally, Fig. 6 depicts the norms of the adaptation signals  $e_{\vartheta_i}(t)$  and  $e_{\vartheta_{O,i}}(t)$ ,  $\forall i \in \{1, 2\}$ , which are bounded in this case as well.

## B. Prescribed Performance Control

In this subsection, we present simulation and experimental results for the control protocol developed in Section IV-B.

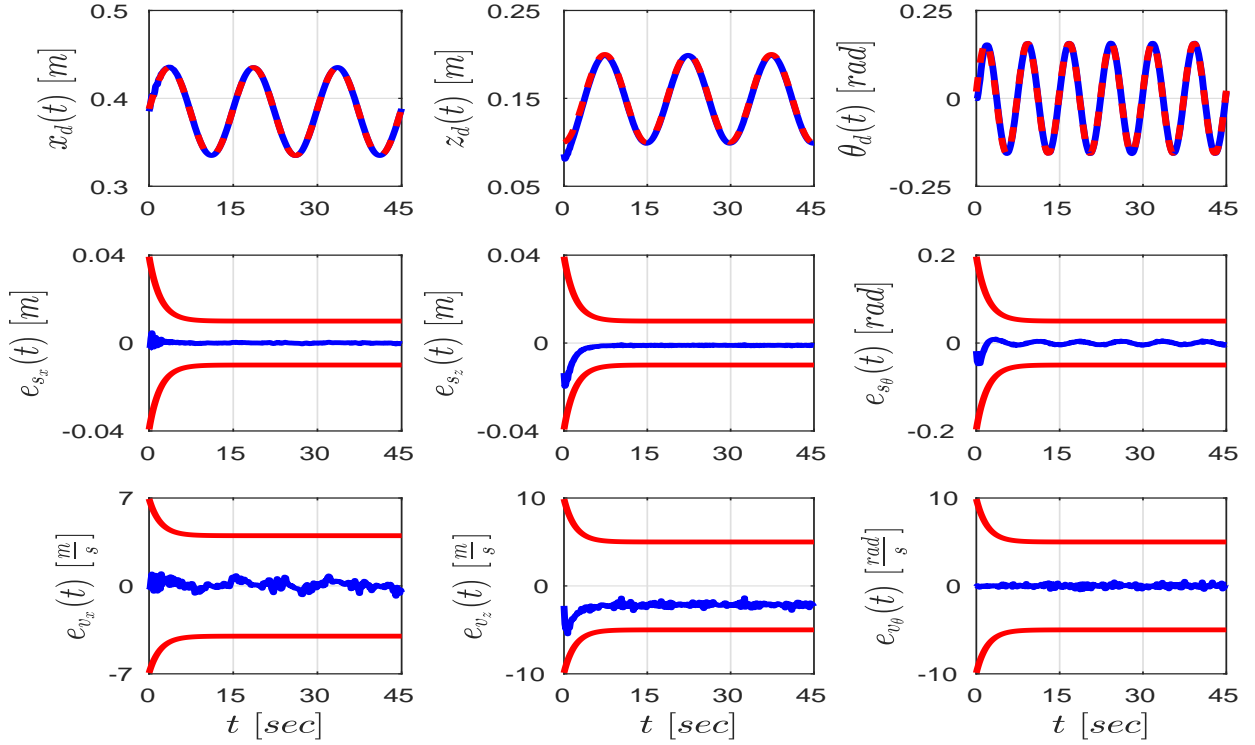


Fig. 9: Simulations results for the controller of subsection IV-B, for  $t \in [0, 45]$  [sec]. Top: The desired (with blue) and actual (with red) object trajectory in  $x$ -,  $z$ -axis, and around  $y$ -axis. Middle: The pose errors  $e_s(t)$  (with blue), as well as the performance functions  $\rho_s(t)$  (with red), respectively. Bottom: The velocity errors  $e_v(t)$  (with blue), as well as the performance functions  $\rho_v(t)$  (with red), respectively.

1) *Simulation Results:* The desired trajectory in this subsection was chosen the same as in subsection V-A1, i.e.,  $x_d(t) = 0.35 + 0.05 \sin(\frac{2\pi t}{15})$  [m],  $z_d(t) = 0.15 - 0.05 \cos(\frac{2\pi t}{15})$  [m], and  $\theta_d(t) = \frac{\pi}{20} \sin(\frac{5\pi t}{15})$  [rad]. The prescribed performance functions are chosen as:  $\rho_{s_x}(t) = \rho_{s_z}(t) = 0.03 \exp(-0.5t) + 0.01$  [m],  $\rho_{s_\theta}(t) = 0.45 \exp(-0.5t) + 0.05$  [rad],  $\rho_{v_x}(t) = 3 \exp(-0.5t) + 4$  [m/s],  $\rho_{v_z}(t) = 5 \exp(-0.5t) + 5$  [m/s], and  $\rho_{v_\theta}(t) = 5 \exp(-0.5t) + 5$  [rad/s]. The simulation results are depicted in Figs. 9 and 10; Fig. 9 shows the desired and actual trajectory of the object's center of mass (top), the pose errors  $e_s(t)$  along with the performance functions  $\rho_s(t)$  (middle), as well as the velocity error  $e_v(t)$  along with the velocity performance functions  $\rho_v(t)$  (bottom). It is verified that we achieve tracking of the desired trajectory with prescribed performance. The control inputs (joint torques) as well as the joint velocities are given in Fig. 10. By following the procedure described in the proof of theorem 3, we tune the gains to the values  $g_s = 0.05$  and  $g_v = 7$  so that the joint torques and velocities respect their respective bounds.

2) *Experimental Results:* We set the desired trajectory in this subsection as in subsection V-A2, i.e.,  $x_d(t) = 0.3 + 0.05 \sin(\frac{2\pi t}{35})$  [m],  $z_d(t) = 0.15 - 0.05 \cos(\frac{2\pi t}{35})$  [m], and  $\theta_d(t) = \frac{\pi}{20} \sin(\frac{5\pi t}{35})$  [rad]. The parameters for the prescribed performance functions are chosen as:  $\rho_{s_x}(t) = \rho_{s_z}(t) = 0.03 \exp(-0.2t) + 0.02$  [m],  $\rho_{s_\theta}(t) = 0.2 \exp(-0.2t) + 0.2$  [rad],  $\rho_{v_x}(t) = 5 \exp(-0.2t) + 5$  [m/s],  $\rho_{v_z}(t) = 5 \exp(-0.2t) + 10$  [m/s], and  $\rho_{v_\theta}(t) = 4 \exp(-0.2t) + 3$  [m/s]. The values for the gains are set at  $g_s = 0.05$  and  $g_v = 6.8$ .

The simulation results are depicted in Figs. 11 and 12; Fig. 11 shows the desired and actual trajectory of the object's center of mass (top), the pose errors  $e_s(t)$  along with the performance functions  $\rho_s(t)$  (middle), as well as the velocity error  $e_v(t)$  along with the velocity performance functions  $\rho_v(t)$  (bottom). The prescribed performance tracking can be verified in the experimental case as well. The control inputs (joint torques) as well as the joint velocities are given in Fig. 12, where it is shown that they respect their corresponding limits.

### C. Discussion

It is clear from the aforementioned figures that the tracking of the desired trajectory is achieved by both controllers in the computer simulation and experimental cases. It is worth noting first the difference between the simulations and experiments, which, for both control protocols, lies in the velocity errors. The latter present some oscillatory behavior in the experimental case, which can be attributed to sensor noise, external disturbances/model uncertainties, or inaccuracies/delays of the internal ArbotiX-M controller. The same reason led us to choose slower desired trajectories for the real-time experiments. Nonetheless, these oscillations do not affect the overall tracking performance; Recall that for the Prescribed Performance Controller, tracking of the desired trajectory does not require the functions  $\rho_{v_k}(t)$  - and hence the velocity errors  $e_{v_k}$ ,  $k \in \mathcal{K}$  - to asymptotically approach zero.

Among the two control schemes, we can notice a slightly more aggressive behavior of the joint velocities and torques for



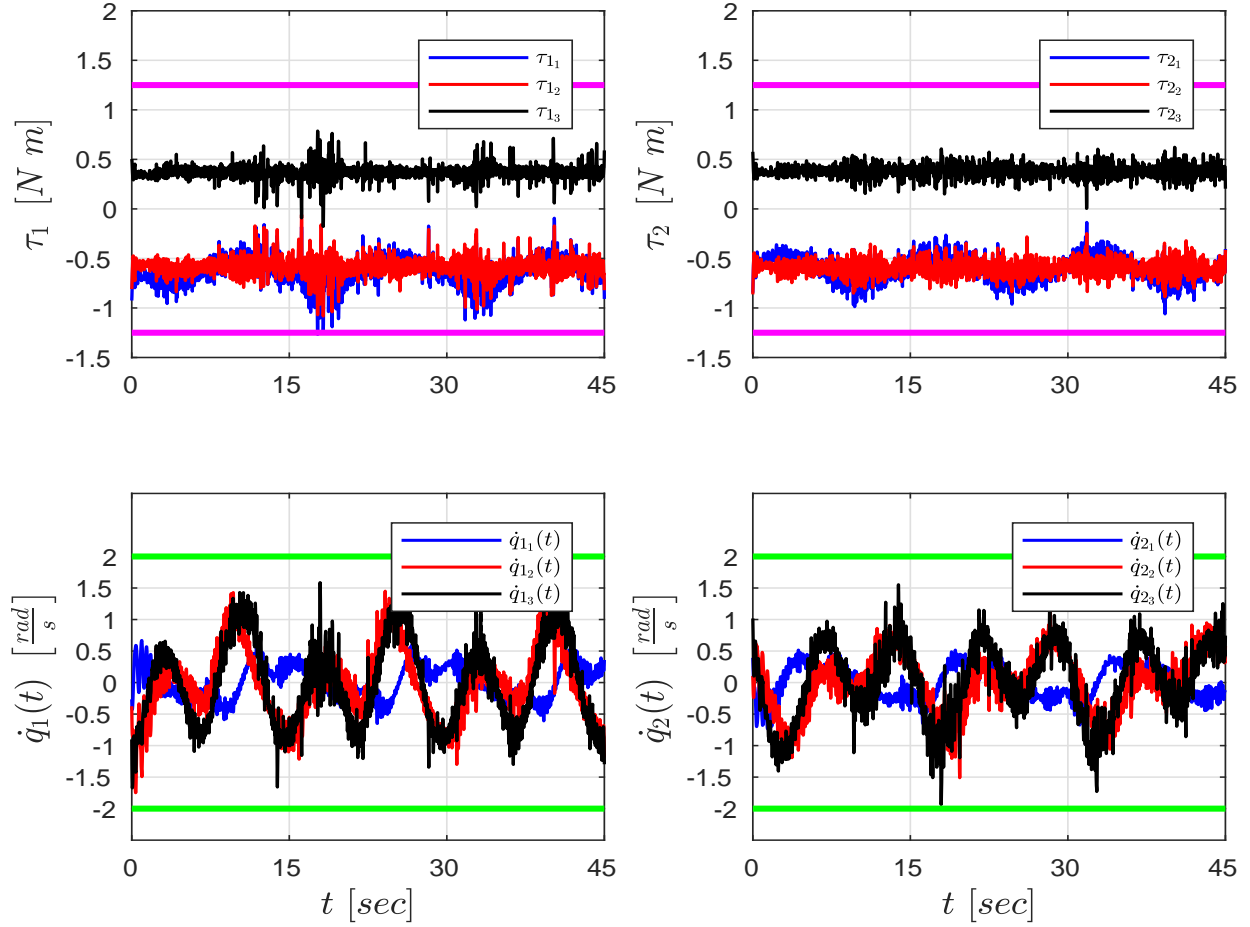


Fig. 10: The agent joint torques and velocities of the simulation of the controller in subsection IV-B, for  $t \in [0, 45]$  [sec], with their respective limits (purple and green lines, respectively). Top: The joint torques of agent 1 (left) and agent 2 (right). Bottom: The joint velocities of agent 1 (left) and agent 2 (right).

the Prescribed Performance Controller, which can be attributed to the virtual force that “pushes” the errors  $e_{s_k}, e_{v_k}$  not to hit the bounds of the performance functions  $\rho_s(t), \rho_v(t)$ , respectively,  $\forall k \in \mathcal{K}$ . Note, however, that this methodology does not require knowledge of the structure of the dynamic terms  $M_i(q_i), C_i(q_i, \dot{q}_i), g_i(q_i)$ , whose derivation can be tedious, and yields thus significantly lower analytic complexity, without sacrificing the actual performance.

## VI. CONCLUSION AND FUTURE WORK

We presented two novel decentralized control protocols for the cooperative manipulation of a single object by  $N$  robotics agents. Firstly, we developed a quaternion-based approach that avoids representation singularities with adaptation laws to compensate for dynamic uncertainties. Secondly, we developed a robust control law that guarantees prescribed performance for the transient and steady state of the object. Both methodologies were validated via realistic simulations and experimental results. Future efforts will be devoted towards applying the proposed techniques to cases with non rigid grasping points as well as uncertain object geometric characteristics.

## REFERENCES

- [1] S. A. Schneider and R. H. Cannon, “Object impedance control for cooperative manipulation: Theory and experimental results,” *IEEE Transactions on Robotics and Automation*, vol. 8, no. 3, pp. 383–394, 1992.
- [2] T. G. Sugar and V. Kumar, “Control of cooperating mobile manipulators,” *IEEE Transactions on robotics and automation*, vol. 18, no. 1, pp. 94–103, 2002.
- [3] O. Khatib, K. Yokoi, K. Chang, D. Ruspini, R. Holmberg, and A. Casal, “Decentralized cooperation between multiple manipulators,” *IEEE International Workshop on Robot and Human Communication*, pp. 183–188, 1996.
- [4] Y.-H. Liu, S. Arimoto, and T. Ogasawara, “Decentralized cooperation control: non-communication object handling,” *Proceedings of the IEEE Conference on Robotics and Automation (ICRA)*, vol. 3, pp. 2414–2419, 1996.
- [5] Y.-H. Liu and S. Arimoto, “Decentralized adaptive and nonadaptive position/force controllers for redundant manipulators in cooperations,” *The International Journal of Robotics Research*, vol. 17, no. 3, pp. 232–247, 1998.
- [6] M. Zribi and S. Ahmad, “Adaptive control for multiple cooperative robot arms,” *Proceedings of the IEEE International Conference on Decision and Control (CDC)*, pp. 1392–1398, 1992.
- [7] J. Gudiño-Lau, M. A. Arteaga, L. A. Munoz, and V. Parra-Vega, “On the control of cooperative robots without velocity measurements,” *IEEE Transactions on Control Systems Technology*, vol. 12, no. 4, pp. 600–608, 2004.
- [8] J. T. Wen and K. Kreutz-Delgado, “Motion and force control of multiple robotic manipulators,” *Automatica*, vol. 28, no. 4, pp. 729–743, 1992.
- [9] T. Yoshikawa and X.-Z. Zheng, “Coordinated dynamic hybrid position/force control for multiple robot manipulators handling one con-

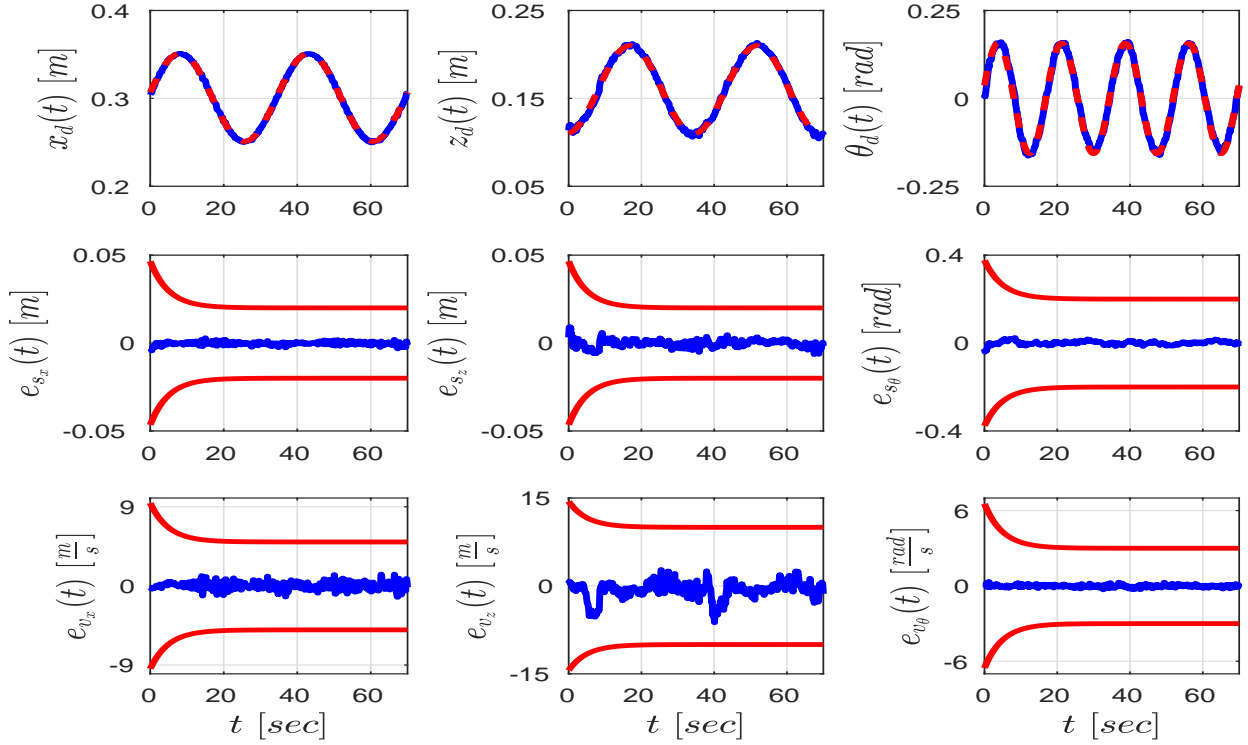


Fig. 11: Experimental results for the controller of subsection IV-B, for  $t \in [0, 45]$  [sec]. Top: The desired (with blue) and actual (with red) object trajectory in  $x$ -,  $z$ -axis, and around  $y$ -axis. Middle: The pose errors  $e_s(t)$  (with blue), as well as the performance functions  $\rho_s(t)$  (with red), respectively. Bottom: The velocity errors  $e_v(t)$  (with blue), as well as the performance functions  $\rho_v(t)$  (with red), respectively.

- strained object,” *The International Journal of Robotics Research*, vol. 12, no. 3, pp. 219–230, 1993.
- [10] C. D. Kopf, “Dynamic two arm hybrid position/force control,” *Robotics and Autonomous Systems*, vol. 5, no. 4, pp. 369–376, 1989.
- [11] F. Caccavale, P. Chiacchio, and S. Chiaverini, “Task-space regulation of cooperative manipulators,” *Automatica*, vol. 36, no. 6, pp. 879–887, 2000.
- [12] F. Caccavale, P. Chiacchio, A. Marino, and L. Villani, “Six-dof impedance control of dual-arm cooperative manipulators,” *IEEE/ASME Transactions On Mechatronics*, vol. 13, no. 5, pp. 576–586, 2008.
- [13] D. Heck, D. Kostić, A. Denasi, and H. Nijmeijer, “Internal and external force-based impedance control for cooperative manipulation,” *Proceedings of the IEEE European Control Conference (ECC)*, pp. 2299–2304, 2013.
- [14] S. Erhart and S. Hirche, “Adaptive force/velocity control for multi-robot cooperative manipulation under uncertain kinematic parameters,” *Proceedings of the IEEE/RSJ International Conference on Intelligent Robots and Systems (IROS)*, pp. 307–314, 2013.
- [15] S. Erhart, D. Sieber, and S. Hirche, “An impedance-based control architecture for multi-robot cooperative dual-arm mobile manipulation,” *Proceedings of the IEEE/RSJ International Conference on Intelligent Robots and Systems (IROS)*, pp. 315–322, 2013.
- [16] Y. Kume, Y. Hirata, and K. Kosuge, “Coordinated motion control of multiple mobile manipulators handling a single object without using force/torque sensors,” *Proceedings of the IEEE/RSJ International Conference on Intelligent Robots and Systems (IROS)*, pp. 4077–4082, 2007.
- [17] J. Szewczyk, F. Plumet, and P. Bidaud, “Planning and controlling cooperating robots through distributed impedance,” *Journal of Robotic Systems*, vol. 19, no. 6, pp. 283–297, 2002.
- [18] A. Tsiamis, C. K. Verginis, C. P. Bechlioulis, and K. J. Kyriakopoulos, “Cooperative manipulation exploiting only implicit communication,” *Proceedings of the IEEE/RSJ International Conference on Intelligent Robots and Systems (IROS)*, pp. 864–869, 2015.
- [19] F. Ficuciello, A. Romano, L. Villani, and B. Siciliano, “Cartesian impedance control of redundant manipulators for human-robot co-manipulation,” *Proceedings of the IEEE/RSJ International Conference on Intelligent Robots and Systems (IROS)*, pp. 2120–2125, 2014.
- [20] A.-N. Ponce-Hinestroza, J.-A. Castro-Castro, H.-I. Guerrero-Reyes, V. Parra-Vega, and E. Olguín-Díaz, “Cooperative redundant omnidirectional mobile manipulators: Model-free decentralized integral sliding modes and passive velocity fields,” *Proceedings of the IEEE International Conference on Robotics and Automation (ICRA)*, pp. 2375–2380, 2016.
- [21] W. Gueaieb, F. Karray, and S. Al-Sharhan, “A robust hybrid intelligent position/force control scheme for cooperative manipulators,” *IEEE/ASME Transactions on Mechatronics*, vol. 12, no. 2, pp. 109–125, 2007.
- [22] Z. Li, C. Yang, C. Y. Su, S. Deng, F. Sun, and W. Zhang, *IEEE Transactions on Fuzzy Systems*, vol. 23, no. 4, pp. 1044–1056, 2015.
- [23] K. Tzierakis and F. Koumboulis, “Independent force and position control for cooperating manipulators,” *Journal of the Franklin Institute*, vol. 340, no. 6, pp. 435–460, 2003.
- [24] A. Marino, “Distributed adaptive control of networked cooperative mobile manipulators,” *IEEE Transactions on Control Systems Technology*, 2017.
- [25] A. Pettiti, A. Franchi, D. Di Paola, and A. Rizzo, “Decentralized motion control for cooperative manipulation with a team of networked mobile manipulators,” *Proceedings of the IEEE International Conference on Robotics and Automation (ICRA)*, pp. 441–446, 2016.
- [26] F. Aghili, “Self-tuning cooperative control of manipulators with position/orientation uncertainties in the closed-kinematic loop,” *2011 IEEE/RSJ International Conference on Intelligent Robots and Systems (IROS)*, pp. 4187–4193, 2011.
- [27] S. Erhart and S. Hirche, “Model and analysis of the interaction dynamics in cooperative manipulation tasks,” *IEEE Transactions on Robotics*, vol. 32, no. 3, pp. 672–683, 2016.
- [28] —, “Internal force analysis and load distribution for cooperative multi-robot manipulation,” *IEEE Transactions on Robotics*, vol. 31, no. 5, pp. 1238–1243, 2015.
- [29] Z. Wang and M. Schwager, “Multi-robot manipulation with no communication using only local measurements,” *Proceedings of the IEEE Conference on Decision and Control (CDC)*, pp. 380–385, 2015.
- [30] L. Chaimowicz, M. F. M. Campos, and V. Kumar, “Hybrid systems modeling of cooperative robots,” *Proceedings of the IEEE International*

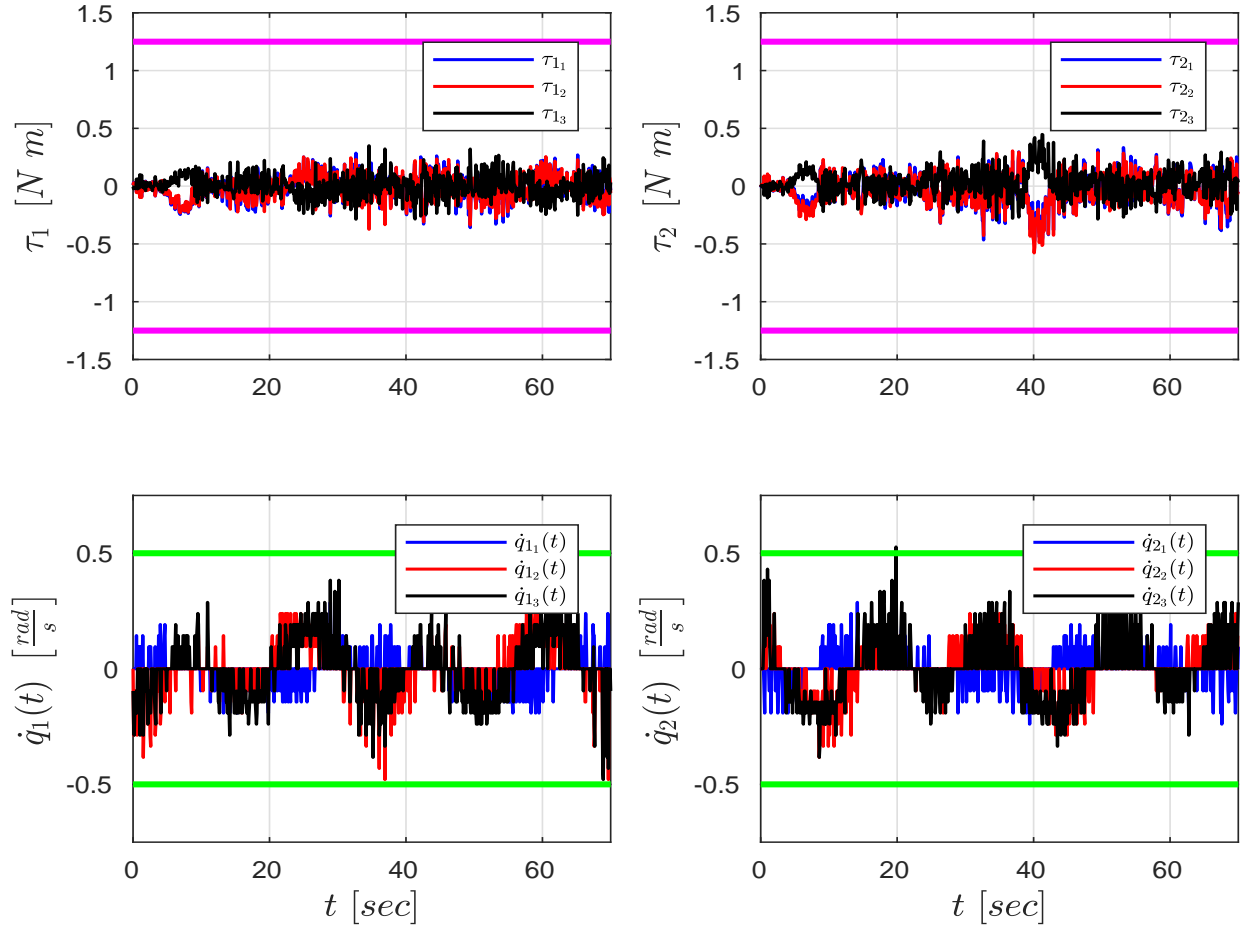


Fig. 12: The agent joint torques and velocities of the experiment of the controller in subsection IV-B, for  $t \in [0, 45]$  [sec], with their respective limits (purple and green lines, respectively). Top: The joint torques of agent 1 (left) and agent 2 (right). Bottom: The joint velocities of agent 1 (left) and agent 2 (right).

- Conference on Robotics and Automation (ICRA), vol. 3, pp. 4086–4091, 2003.
- [31] T. D. Murphey and M. Horowitz, “Adaptive cooperative manipulation with intermittent contact,” *Proceedings of the IEEE International Conference on Robotics and Automation (ICRA)*, pp. 1483–1488, 2008.
- [32] Z. Wang and M. Schwager, “Kinematic multi-robot manipulation with no communication using force feedback,” *Proceedings of the IEEE International Conference on Robotics and Automation (ICRA)*, pp. 427–432, 2016.
- [33] H. Bai and J. T. Wen, “Cooperative load transport: A formation-control perspective,” *IEEE Transactions on Robotics*, vol. 26, no. 4, pp. 742–750, 2010.
- [34] H. G. Tanner, S. G. Loizou, and K. J. Kyriakopoulos, “Nonholonomic navigation and control of cooperating mobile manipulators,” *IEEE Transactions on Robotics and Automation*, vol. 19, no. 1, pp. 53–64, 2003.
- [35] A. Nikou, C. K. Verginis, S. Heshmati-alamdari, and D. V. Dimarogonas, “A nonlinear model predictive control scheme for cooperative manipulation with singularity and collision avoidance,” *Mediterranean Conference on Control and Automation*, 2017.
- [36] C. K. Verginis, M. Mastellaro, and D. V. Dimarogonas, “Robust quaternion-based cooperative manipulation without force/torque information,” *World Congress of the International Federation of Automatic Control*, 2017.
- [37] B. Siciliano, L. Sciacivco, L. Villani, and G. Oriolo, *Robotics: modelling, planning and control*. Springer Science & Business Media, 2010.
- [38] C. P. Bechlioulis and G. A. Rovithakis, “A low-complexity global approximation-free control scheme with prescribed performance for unknown pure feedback systems,” *Automatica*, vol. 50, no. 4, pp. 1217–1226, 2014.
- [39] E. D. Sontag, *Mathematical control theory: deterministic finite dimensional systems*. Springer Science & Business Media, 2013, vol. 6.
- [40] R. Campa, K. Camarillo, and L. Arias, “Kinematic modeling and control of robot manipulators via unit quaternions: Application to a spherical wrist,” *Proceedings of the IEEE Conference on Decision and Control (CDC)*, pp. 6474–6479, 2006.
- [41] J.-J. E. Slotine and W. Li, “On the adaptive control of robot manipulators,” *The International Journal of Robotics Research*, vol. 6, no. 3, pp. 49–59, 1987.
- [42] J.-J. E. Slotine, W. Li *et al.*, *Applied nonlinear control*. prentice-Hall Englewood Cliffs, NJ, 1991, no. 1.
- [43] S. P. Bhat and D. S. Bernstein, “A topological obstruction to continuous global stabilization of rotational motion and the unwinding phenomenon,” *Systems & Control Letters*, vol. 39, no. 1, pp. 63–70, 2000.
- [44] C. G. Mayhew, R. G. Sanfelice, and A. R. Teel, “Quaternion-based hybrid control for robust global attitude tracking,” *IEEE Transactions on Automatic Control*, vol. 56, no. 11, pp. 2555–2566, 2011.
- [45] T. Lee, M. Leok, and N. H. McClamroch, “Control of complex maneuvers for a quadrotor uav using geometric methods on  $se(3)$ ,” *arXiv:1003.2005*, 2010.
- [46] E. Rohmer, S. P. Singh, and M. Freese, “V-rep: a versatile and scalable robot simulation framework,” *Proceedings of The International Conference on Intelligent Robots and Systems (IROS)*, 2013.
- [47] Trossenrobotics, “Widowx robot arm kit w/ros.” [Online]. Available: [www.trossenrobotics.com/widowxrobotarm](http://www.trossenrobotics.com/widowxrobotarm)
- [48] Robotis, “Dynamixel actuators.” [Online]. Available: [www.robotis.us/dynamixel](http://www.robotis.us/dynamixel)
- [49] Trossenrobotics, “Arbotix-m robocontroller.” [Online]. Available: <http://www.trossenrobotics.com/p/arbotix-robot-controller.aspx>